END

DATE
FILMED

8 -77

AFAPL-TR-76-102

DEVELOPMENT OF LIGHTWEIGHT TRANSFORMERS FOR AIRBORNE HIGH POWER SUPPLIES

THERMAL TECHNOLOGY LABORATORY INC.
422 NIAGARA FALLS BLVD.
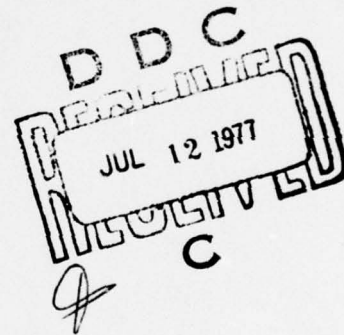*BUFFALO, NEW YORK 14223*

DECEMBER 1976

TECHNICAL REPORT AFAPL-TR-76-102
INTERIM REPORT FOR PERIOD JANUARY 1976 THROUGH JUNE 1976

Prepared for
AIR FORCE AERO PROPULSION LABORATORY
AIR FORCE WRIGHT AERONAUTICAL LABORATORIES
AIR FORCE SYSTEMS COMMAND
WRIGHT-PATTERSON AIR FORCE BASE, OHIO 45433

NOTICE

When Government drawings, specifications, or other data are used for any pur-
pose other than in connection with a definitely related Government procurement
operation, the United States Government thereby incurs no responsibility nor any
obligation whatsoever; and the fact that the Government may have formulated, fur-
nished, or in any way supplied the said drawings, specifications, or other data, is
not to be regarded by implication or otherwise as in any manner licensing the
holder or any other person or corporation, or conveying any rights or permission
to manufacture, use, or sell any patented invention that may be related thereto.
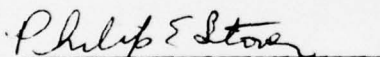
This interim report was submitted by Thermal Technology Laboratory, Inc.,
under Contract F33615-75-C-2014. The effort was sponsored by the Air Force Aero-
Propulsion Laboratory, Air Force Systems Command, Wright-Patterson AFB, Ohio under
Project 3145, Task 32, and Work Unit 05 with Mr. Michael P. Dougherty, AFAPL/POD-1
as project engineer. Mr. James P. Welsh of Thermal Technology Laboratory, Inc.
was technically reponsible for the work.

This report has been reviewed by the Information Office (ASD/OIP) and is
releasable to the National Technical Information Service (NTIS). At NTIS, it
will be available to the general public, including foreign nations.

This technical report has been reviewed and is approved for publication.

MICHAEL P. DOUGHERTY
Project Engineer

FOR THE COMMANDER

PHILIP E. STOVER
Chief, High Power Branch

Copies of this report should not be returned unless return is required by
security considerations, contractual obligations, or notice on a specific document.

AIR FORCE - 8 JUN 77 - 115

SECURITY CLASSIFICATION OF THIS PAGE *(When Data Entered)*

REPORT DOCUMENTATION PAGE		READ INSTRUCTIONS BEFORE COMPLETING FORM
1. REPORT NUMBER AFAPL-TR-76-102	2. GOVT ACCESSION NO.	3. RECIPIENT'S CATALOG NUMBER
4. TITLE *(and Subtitle)* DEVELOPMENT OF LIGHTWEIGHT TRANSFORMERS FOR AIRBORNE HIGH POWER SUPPLIES.		5. TYPE OF REPORT & PERIOD COVERED Interim Report. Jan 75 – June 76,
		6. PERFORMING ORG. REPORT NUMBER
7. AUTHOR(s) Dr. D. L. Lockwood Mr. R. I. McNall, Jr. Mr. R. L. Haumesser		8. CONTRACT OR GRANT NUMBER(s) F33615-75-C-2014
9. PERFORMING ORGANIZATION NAME AND ADDRESS Thermal Technology Laboratory, Inc. 422 Niagara Falls Blvd. Buffalo NY 14223		10. PROGRAM ELEMENT, PROJECT, TASK AREA & WORK UNIT NUMBERS Program Element 62203F Work Unit 31453205
11. CONTROLLING OFFICE NAME AND ADDRESS Air Force Aero-Propulsion Laboratory/POD Wright-Patterson AFB Ohio 45433		12. REPORT DATE December 1976
		13. NUMBER OF PAGES 82
14. MONITORING AGENCY NAME & ADDRESS*(if different from Controlling Office)*		15. SECURITY CLASS. *(of this report)* UNCLASSIFIED
		15a. DECLASSIFICATION/DOWNGRADING SCHEDULE
16. DISTRIBUTION STATEMENT *(of this Report)* Approved for public release; distribution unlimited.		
17. DISTRIBUTION STATEMENT *(of the abstract entered in Block 20, if different from Report)*		
18. SUPPLEMENTARY NOTES		

19. KEY WORDS *(Continue on reverse side if necessary and identify by block number)*

Airborne Transformers
Low Specific Weight Transformers
High Voltage, High Power Transformers
High Energy Density Transformers
Lightweight Transformers

20. ABSTRACT *(Continue on reverse side if necessary and identify by block number)*

Several major developments have occurred in this program. As is often the case in research, they did not occur exactly in accordance with the original plan. The total program however is essentially on schedule.

New techniques for fabrication of pie wound transformers were developed which yielded superior designs. This development was followed by the development of computer aided design programs for pie wound transformers. Several 10KW transformers have been fabricated and subjected to a variety of tests.

DD FORM 1 JAN 73 **1473** EDITION OF 1 NOV 65 IS OBSOLETE

SECURITY CLASSIFICATION OF THIS PAGE *(When Data Entered)*

390 518

Based on the results of these tests both the 10KW and 200 KW transformers will be pie rather than layer wound. A 10KW transformer rectifier system is presently being integrated with a breadboard inverter for final verification.

During the first half of this program, a numerical method was developed for the solution of the nonlinear lumped parameter transformer model. This model was developed under the previous contract, but no stable solution had been found. The present solution is for a resistive load and work is continuing to include leakage inductance, shunt capacitance, and an arbitrary load impedance. The present program has been implemented on the HP 9830 machine.

As mentioned above, pie wound transformer design programs have been written. These are for interactive design on the HP 9830 and are not self optimizing routines. A decision should be made as to the ultimate application of these programs before a decision whether or not to implement them on the CDC 6600.

The materials studies support of the 200KW transformer task are completed with exception of evaluation of some of the newer fluorine based dielectric fluids. Preliminary designs indicate specific weights in the neighborhood of 0.05 lb/KVA for these transformers. Consideration is presently being given to increasing the operating temperature in order to reduce heat exchanger weight.

In support of the general materials studies, several improvements were made in the magnetic core model which permit accurate simulation of hysteresis and I-V curves for most core materials. The model has been compared to existing models and found to be superior in both simplicity and accuracy in all cases.

Computer aided design of transformers is facilitated through two transformer design optimization programs, TRANSOP and TDOP2. Additional work is planned to improve their versatility and usefulness by including some of the newer transformer configurations, i.e., pie windings and magnetic shunts. Improvements in ease of utilization, computational efficiency, and documentation are also planned.

TABLE OF CONTENTS

Pg.

iii

LIST OF ILLUSTRATIONS

LIST OF ILLUSTRATIONS Cont'd

LIST OF TABLES

SECTION II

Introduction and Summary

Thermal Technology Laboratory, Inc. under the USAF Contract F33615-75-C-2014 is performing a comprehensive analytical and experimental program to develop design techniques, experimental high power low specific weight transformer systems, and high power lightweight DC to DC converter system test beds. The effort consists of the following: (1) the development of a 10 KVA inverter transformer suitable for development elsewhere of experimental converter circuits and systems, (2) the refinement of the real time models and computer design optimization programs for inverter, pulse, and sinusoidal waveshape transformers, (3) the development of two experimental 200 KVA inverter transformer systems, (4) the design, fabrication, and testing of two 200 KVA converter system test beds, (5) the design and fabrication of a high voltage non-inductive load for testing the converters. These tasks are summarized below.

In Task 1, a ten (10) KVA experimental inverter transformer has been designed to Government furnished requirements, assembled, and subjected to preliminary tests. A second set of windings have been provided for experimentation and the computer program is being modified, to correlate with the measured electrical performance of the transformer.

In Task 2, the inverter, pulse, and real time models of the transformer are being refined by generalizing the steady state and real time models; determining and implementing a program procedure which will accomodate both models; developing an improved computer aided system for design optimization, and programing on site the WPAFB CDC 6600 computer.

In Task 3, two 200 KVA inverter transformer systems will be designed, fabricated and tested in conformance with requirements provided by the Government. Materials compatability tests will be conducted and special cooling systems designed to match the transformer parameters. One transformer will be designed to work with SCR type

1

inverters and the other designed to work with plasma
switch inverters.

In Task 4, two complete operational 200 KVA converter
test beds will be designed, fabricated, and tested in
accordance with the requirements to be provided by the
Government. One converter will utilize SCR's and the
other plasma switches. A packaging philosophy will be
developed and implemented in the electrical, thermal,
and mechanical designs. Emphasis will be placed on
safety, minimum weight, thermal and electrical performance.
A detailed test plan will be submitted prior to testing.

In Task 5, a noninductive load for testing the
converters will be designed, fabricated, and tested. The
load will be designed to minimize changes in performance
due to varying duty cycles and input powers. Safety, and
electrical and thermal performance will be emphasized.

Summary

Several major developments have occurred in this
program. As is often the case in research, they did
not occur exactly in accordance with the original plan.
The total program however is essentially on schedule.

New techniques for fabrication of pie wound
transformers were developed which yielded superior designs.
This development was followed by the development of computer
aided design programs for pie wound transformers. Several
10KW transformers have been fabricated and subjected to a
variety of tests. Based on the results of these tests both
the 10KW and 200 KW transformers will be pie rather than
layer wound. A 10KW transformer rectifier system is
presently being integrated with a breadboard inverter for
final verification.

During the first half of this program, a numerical
method was developed for the solution of the nonlinear
lumped parameter transformer model. This model was

developed under the previous contract but no stable solution had been found. The present solution is for a resistive load and work is continuing to include leakage inductance, shunt capacitance, and an arbitrary load impedance. The present program has been implemented on the HP 9830 machine.

As mentioned above, pie wound transformer design programs have been written. These are for interactive design on the HP 9830 and are not self optimizing routines. A decision should be made as to the ultimate application of these programs before a decision whether or not to implement them on the CDC 6600.

The materials studies support of the 200KW transformer task are completed with exception of evaluation of some of the newer fluorine based dielectric fluids. Preliminary designs indicate specific weights in the neighborhood of 0.05 lb/KVA for these transformers. Consideration is presently being given to increasing the operating temperature in order to reduce heat exchanger weight.

In support of the general materials studies, several improvements were made in the magnetic core model which permit accurate simulation of hysteresis and I-V curves for most core materials. The model has been compared to existing models and found to be superior in both simplicity and accuracy in all cases.

Computer aided design of transformers is facilitated through two transformer design optimization programs, TRANSOP and TDOP2. Additional work is planned to improve their versatility and usefulness by including some of the newer transformer configurations, i.e., pie windings and magnetic shunts. Improvements in ease of utilization, computational efficiency and documentation are also planned.

3

SECTION III

Technical Discussion

3.1 Summary of capabilities of original program (TRANSOP)

The original computer program developed under Contract
F33615-72-C-1944 for computer aided transformer design
optimization was documented in report No. AFAPL-TR-75-15,
Volume II, "Final Technical Report on Development of
Lightweight Transformers for Airborne High Power Supplies,
Computer Users Manual". The program consisted of a
procedure, FUNCTION TDP, and its associated subroutines
and functions, which determined a consistent set of
dependent design parameter values for a given set of
independent design parameters. In addition, the program
contained a driver procedure, PROGRAM TDPLOT, to aid in
optimizing transformer designs. This procedure read
control and independent design parameter value data from
an appropriate input file and generated corresponding
outputs. The outputs are in the form of 3-dimensional
line printer and/or Cal-Comp plots of the user defined
objective function versus two of the independent design
parameters being optimized. Also, a listing of the final
(optimized) transformer design parameter values are
computed by FUNCTION TDP. A procedure, PROGRAM TERMOP,
was developed to facilitate utilization of PROGRAM TDPLOT
from a remote time share terminal. This program prompts
for appropriate free formatted control and independent
design parameter data input and generated the necessary
control and input data card images on a file for submission
to the REMOTE INPUT FILE as an INTERCOM BATCH job. Output
resulting from execution of PROGRAM TDPLOT as an INTERCOM
BATCH job can be listed at a remote time share terminal or
ROUTED to a batch site printer.

FUNCTION TDP designs 3-phase layer wound, vaporization
cooled rectangular-crossection, C-core transformers. The
user must specify: (1) the conductor cooling rates or
standard wire gauge (AWG), (2) core lamination width,
(3) core lamination thickness, (4) core lamination
insulation thickness, (5) number of inside core laminations,
(6) number of outside core laminations, (7) insulation
dielectric strength, (8) delta or wye connected primary

4

and secondary windings, (9) the number of inside
secondary winding layers, (10) coolant boiling
temperature, (11) coolant vaporization cooling
coefficient and exponent, (12) conductor insulation
thicknesses, (13) insulation thermal resistivity
coefficients, (14) resistivity temperature coefficients
and zero degree centigrade resistivities (15) core spacing
factor, (17) densities, (18) primary and secondary,
line-to-line full load emf, (19) operating frequency,
(20) coolant heat of vaporization, (21) hysteresis dissipation
coefficient and exponent for the Steinmetz relationship,
(22) maximum number of convergence iterations, (23) full-load
output power, (24) eddy-current dissipation coefficient,
(25) core saturation flux density, (26) cooling spacing
factors, (27) minimum spacings, (28) enclosure thickness,
(29) enclosure cooling rate, and (30) whether conductors
are cooled on both or one side. The function initially
assumes that the transformer efficiency is 100% and
iteratively converges on the actual efficiency to within
a specified error. The function then computes the
remaining 300 transformer design parameters.

The major advantage of the TRANSOP program is its
ability to provide visual information on parametric
relationships in the form of plots. Another useful
capability is its ability to consider non standard
transformer designs having different size inner and outer core
leg cross-sectional   areas and different inner and outer
core leg winding wire sizes. The large number of parameters
make it possible to consider and analyze many other
transformer design parameter characteristics.

Unfortunately, such detail makes the program quite
large with a tendency to be time consuming and laborious
to utilize. This subsequently lead to the development of
much simpler and easier to use interactive programs in
HP-BASIC to run on an HP-9830 A programmable calculator.

3.1.2 New Transformer Design Optimization, Program II (TDOP2)

A second transformer design optimization program (TDOP2) has been implemented on CDC-6000 series computing systems in Extended FORTRAN. This is a translated and highly modified version of a simpler and correspondingly less versatile program previously implemented in BASIC on an HP-9830. TDOP2 allows ranging of specified transformer parameters over specified ranges (e.g., core area, conductor size, number of primary and secondary layers, etc.) For each combination of ranged parameter values (along with the fixed input parameters), the program computes the design properties of a transformer by means of an iterative convergent efficiency computation. In addition, bounds may be set on derived transformer parameters (e.g., minimum efficiency, maximum per unit resistance and reactance, one or more physical dimensions, etc.).

3.1.2.1 Transformer Design Capabilities

Transformer design parametric relationships incorporated in to TDOP2 include:

Leakage Inductance

A standard approximation for calculating leakage inductance L of a transformer, referenced to a secondary winding of N turns is:

$$L = 32 M_c N^2 \ell^{-1} m^{-2} 10^{-9} \left(nd + t/3 \right) \qquad \text{henries} \qquad (1)$$

where

N = Number of turns in secondary winding
M_c = Mean circumference of primary + secondary winding (inches)
l = Height of cylinder type coil (inches)
n = Number of interleavings of primary and secondary layers
d = Distance between primary and secondary layers (inches)
t = Primary + secondary winding thickness (inches)

This formula has been verified for accuracy in previous transformer designs, and is used in the program.

The corresponding leakage reactance in ohms, X_L, is given by:

$$X_L = 2\pi f L \tag{2}$$

where f = operating frequency, Hertz

The leakage reactance on a per unit basis, X_L is given by:

$$X_L' = 3 X_L I_s^2 / P_o \tag{3}$$

where I_s = secondary winding current, ohms
       P_o = output power, watts

In general, the leakage reactance of most designs could be maintained at about 0.02-0.03 by maximizing the number of interleavings, n .

Per Unit Resistance

The program computes the total dissipation (copper loss) P_c in watts per coil by

$$P_c = I_p^2 R_p + I_s^2 R_s \tag{4}$$

Where I_p = primary winding current, amperes
       R_p = primary resistance, ohms
       I_s = secondary winding current, amperes
       R_s = secondary resistance, ohms

The computed resistance values include both AC resistivity and temperature coefficient of resistivity effects.

The per unit resistance, R, is given by

$$R = 3 P_c / P_o \tag{5}$$

7

In general, as the unit surface cooling rate increases, the per unit resistance increases. A limitation on maximum per unit resistance can prevent utilization of very high unit surface cooling rates. This factor can lead to the ultimate selection of forced oil cooling over vaporization cooling, when very high unit surface cooling rates are not required.

Primary-to-secondary interleaving

The primary effect of an increased number of primary to secondary interleavings is to reduce the leakage inductance. The program assumes that for a given number of primary and secondary layers, the coils will be arranged so as to maximize the number of interleavings.

AC Resistivity Effects

As conductor diameter and operating frequency increase, skin effects become more pronounced. The net result is that for a given conductor diameter, the apparent resistance of the conductor is greater at high frequencies than the D.C. resistance. The published tabulated data for this AC resistivity increase were fitted to the equation

$$R_{AC}/R_{DC} = 0.9908 + 0.1768 \left[(x - 2.11) + \sqrt{(x - 2.11)^2 + 0.283} \right] \quad (6)$$

where

R_{AC}/R_{DC} = resistance ratio, AC to DC
$\quad x$ = 0.271767 $d \sqrt{f}$ (for copper conductors only)
$\quad d$ = conductor diameter, inches
$\quad f$ = operating frequency, hertz

The relationship is theoretically valid only for isolated conductors, but it has been applied to the side-by-side conductor situation existing in a transformer coil. The effect has been included in the program.

8

Duty Cycle

Duty cycle has a significant effect on the choice
of cooling system and the resultant overall system size
and weight. For very low duty cycle operation an
adiabatic system (no explicit cooling system) can be
constructed with adequate thermal capacity and with
reasonably sized cores and conductors. Because there
are no external cooling system components, this system
can have decided size and weight advantages. Such a
system, however, may not meet higher duty cycle requirements
and active cooling systems would have to be employed. The
effects of thermal capacity on necessary cooling rates is
considered in the program for any noncontinuous duty
transformer.

Load Voltage

The necessary full load secondary rms line-to-line
emf is equal to 0.74 for a Three-Phase Bridge or 1.11 for
a Single-Phase Bridge times the average bridge rectifier
dc output emf divided by the cosine of the value of .694
times the commutation overlap angle, i.e.

$$E_{SL} = 0.74 * E_o / \cos(0.694 * \alpha) \qquad 3\text{-}PHASE \qquad (7a)$$

$$E_{SL} = 1.11 * E_o / \cos(0.694 * \alpha) \qquad 1\text{-}PHASE \qquad (7b)$$

where

E_{SL} and E_O are in equal units and α is in radians.

The full load secondary rms winding emf is equal to
the line-to-line emf for single-phase and 3-phase delta
connected secondary and to the line-to-line emf divided
by the square root of 3 for a y connected secondary, i.e.

9

$$E_{sw} = E_{sll} \qquad : \triangle \, \& \, SINGLE \, PHASE \qquad (8a)$$

$$E_{sw} = E_{sll} / \sqrt{3} \quad : Y \qquad (8b)$$

Load Current

The secondary rms line current is equal to 0.816 for a Three-Phase Bridge or 1.00 for a Single-Phase Bridge times the average bridge rectified dc output current times the rms load current waveform factor, i.e.

$$I_{sl} = 0.816 * I_0 * F_l \qquad 3\text{-}PHASE \qquad (9a)$$

$$I_{sl} = 1.00 * I_0 * F_l \qquad 1\text{-}PHASE \qquad (9b)$$

where
I_{SL} and I_O are in equal units and
F_L = 1.11 for half wine wave load current waveforms
     = 1.04 for semi square wave load current waveforms
     = 1.00 for a constant DC load

The rms secondary winding current is equal to the rms line current for Single-Phase and 3-Phase wYe connected secondary and to the rms line current divided by the square root of 3 for a delta connected secondary, i.e.

$$I_{sw} = I_{sl} \quad : Y \qquad (10a)$$

$$I_{sw} = I_{sl} / \sqrt{3} \quad : \triangle \qquad (10b)$$

3.1.2.2 Surface Cooling Rates & Cooling System Descriptions

Attainable surface cooling rates (cores, conductors, rectifiers plates) are a function of the cooling system under consideration.

Three basic methods of cooling can be specified. Natural convection cooling relationships are presently not included in the program. The rate of heat removal by liquid natural convection is very low (on the order of 0.1 watts/(sq.in-C). A brief description of the physical aspects of each system follows.

Vaporization Cooling

In a vaporization cooled transformer, the coil assemblies are formed in concentric layers, with annular cooling passages between layers. When immersed in a low boiling point coolant, such as Freon 113 or 3 M's FC 78, the Joulean heat raises the coil temperature, the coolant at the coil surface boils, and the vapor escapes through the cooling passage by natural bouyancy forces. The heat of vaporization of the fluid, combined with the agitation resulting from vapor bubble flow, results in the capability of extremely high heat transfer rates at the conductor surface. The generated vapor must either be expended or condensed and returned to the system. Cost, logistic, and environmental conditions must be considered. The volume and weight of a condenser whose capacity matched the on time dissipation rate would generally be large, even if thermal capacity is included. The use of a smaller capacity condenser (one whose capacity equals or exceeds the dissipation rate averaged over an entire cycle, including off time) requires a vapor storage facility. An accumulator could be used for this purpose, maintaining an essentially constant pressure system, but the vapor generation rate generally requires too great a volume to be practical. For example, a 3 MW transformer dissipating 45 KW (98.5% efficient) using an F113 vaporization cooling system would generate approximately 22 cubic feet of vapor during each 15 seconds of operation, ignoring thermal capacity effects and heat transfer to the environment.

11

The alternative to a constant pressure accumulator cooling system is a constant volume system, wherein the system vapor pressure is allowed to vary with the fluid temperature; that is, the system pressure is always the vapor saturation pressure corresponding to the fluid temperature, and incipient boiling conditions always prevail. The physical housing of such a system including the case and all case seals, penetrations, and gasketed joints, must be designed to withstand the maximum internal pressure anticipated, as well as the possibility of negative internal pressure during low temperature non-operating conditions.

Vaporization cooling is capable of unit surface cooling rates of 1.0 to 50.0 watts/(sq in-C). Use of the higher end of the range of cooling rates available with this system may lead to system efficiencies below the minimum acceptable value for some applications. Consequently, full use may not be made of this cooling capability to achieve minimum size and weight.

Adiabatic System

An adiabatic system relies solely on the thermal capacitance of the system elements to absorb the dissipated heat without excessive temperature rise. No explicit heat transfer to the environment is included; rather, it is assumed that the off time between operating intervals is long enough to ensure stabilization of the equipment at or near ambient temperatures prior to the next operating interval, by natural modes of conduction, free convection, and radiation.

The obvious advantage of the adiabatic system is the weight and volume saving associated with the absence of any explicit cooling system. Conductor sizes in adiabatic systems tend to be larger than those in systems employing explicit cooling means, the overall weight of the transformer is greater, but system weight can be less, since a cooling system is not required. Rectifiers in an adiabatic system must be provided with a heat absorbing sink in the form of a metal plate of sufficient thermal capacity.

12

Surface cooling rates are so low that for practical
purposes, they may be assumed to be zero. Dissipative
elements must be designed to have sufficient thermal
capacity to absorb the generated heat during an operating
interval with an acceptable temperature rise. These
systems are generally suitable for total on time within
an operating interval of about 60 seconds or less. The
time between operating intervals must be on the order of
24 hours or more to allow a sufficient cooling down period.

Forced Liquid Cooled Systems

Forced oil cooling systems provide a compromise
between vaporization cooled systems and adiabatic systems.
Vaporization cooled systems provide a very high heat
transfer capability, but require a cooling   system
carefully designed for each application.   Adiabatic
systems provide a very low thermal capability, but do so
with extreme physical simplicity. Forced oil cooled
systems provide a moderate thermal capability, using
cooling system components which are usually somewhat smaller
than for vaporization cooling but also require a pump and
motor. The tradeoffs must be evaluated.

A forced oil system is physically similar in
construction to a vaporizatinn cooled system, although
actual dimensions may differ. Coil assemblies are formed
in concentric layers, with annular cooling spaces between
layers. The coolant is an oil chosen on the basis of
thermodynamic properties, dielectric breakdown characteristic,
cost and availability, and other pertinent factors. The
coolant is forced through the cooling spaces by an external
pump. The transformer design must minimize flow paths
in parallel with the cooling spaces and must ensure an
adequate oil flow velocity in each channel and in all
portions of a given channel.

Forced liquid cooling is capable of unit surface
cooling rates of 0.1 to 1.0 watts/(sq in $^{\circ}$ C), dependent on
the thermodynamic properties of the fluid coolant and on
the coolant velocity. Coolant flow rate must be correlated
with the head-flow characteristics of the available pumps,
and with total system pressure drop, including external

13

heat exchanger. The available cooling rates for moderate flow rates of a typical transformer oil can be compatable with the required system characteristics and minimum weight and volume.

Forced Air Cooling

Forced liquid cooling relationships are also characteristic of a forced gas cooled system when gas compression is not significant.

Forced air cooling, using ambient air blown through an open coil transformer structure and an open rectifier bank, can achieve cooling rates in excess of 0.1 watts/(sq in-C), and requires only a blower and filter as an external cooling system. When very high voltages are involved, this type cooling system may not be acceptable on the basis of safety and contamination with subsequent breakdown.

3.1.3 Transformer Design Optimization Function Considerations

The obvious and usually specified objective function for a design optimization is the transformer weight. This specification usually arises because the design optimization of the overall system is broken into sections which include the design optimization of subsystems with the transformer being treated as an individual component whose weight adds to the total weight of the system. Therefore, by minimizing the weight of each subsystem component the overall system weight would be minimized. It is believed that the preceeding is not necessarily a valid assumption. It appears that if a minimum weight optimization of the overall system design is carried out on the overall integrated system, the resulting optimal transformer design may not be a minimum weight transformer. Therefore, transformer weight is not necessarily a suitable transformer design optimization objective function in itself.

systems designed to match the transformer parameters.
One transformer will be designed to work with SCR type

1

To support the preceding statements and derive a suitable objective function for minimizing the overall system weight, the following general analysis of a representative system is presented.
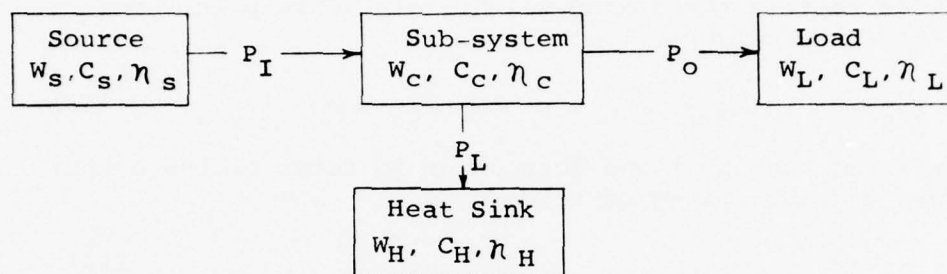
Fig. 3-1

Minimum Weight System Block Diagram

Fig. 3-1 is a block diagram representation of a sub system interconnected to the remainder of a system whose overall weight is to be minimized, where:

P_I = input power to sub system
P_O = useful output power from sub-system
P_L = sub system power losses

W_y = weight
C_y = specific weight
η_y = efficiency

X_S = source
X_C = sub system (component)
X_L = load
X_H = heat sink

The total system weight W_T is equal to the sum of the weights of the sub systems, i.e.

$$W_T = W_S + W_C + W_L + W_H \qquad (11)$$

15

Substituting for the sub-system weights their corresponding specific weight and power, i.e.

$$W = C * P \tag{12}$$

We can rewrite the system weight relationship in terms of specific weights, i.e.

$$W_T = C_S * P_I + C_C * P_O + C_L * P_O + C_H * P_L \tag{13}$$

Rewriting the input and loss power in terms of the output power and sub system efficiency, i.e.

$$P_I = P_O / \eta_C \tag{14}$$

$$P_L = P_O \left(\frac{1}{\eta_C} - 1 \right) \tag{15}$$

Substituting, the total system weight equation now becomes

$$W_T = C_S * P_O / \eta_C + C_C * P_O + C_L * P_O + C_H * P_O * \left(-1 + \frac{1}{\eta_C} \right) \tag{16}$$

Dividing through by the sub-system output power we have a resulting relationship for the specific weight of the total system, i.e.

$$C_T = \frac{W_T}{P_O} = \frac{C_S}{\eta_C} + C_C + C_L + C_H * \left(\frac{1}{\eta_C} - 1 \right) \tag{17}$$

The individual specific weights can be represented as ratios of the specific weight of the sub-system of interest, i.e.

$$C_S = R_S * C_C \tag{18a}$$
$$C_L = R_L * C_C \tag{18b}$$
$$C_H = R_H * C_C \tag{18c}$$

The specific weight of the total system can now be specified in terms of the specific weight and efficiency of the sub-system of interest and the ratio of all other specific weights to it i.e.,

$$C_T = \frac{R_s C_c}{\eta_c} + C_c + R_L C_c + R_H C_c \left(-1 + \frac{1}{\eta_c}\right) \qquad (19)$$

Factoring out C_c:

$$C_T = C_c * \left(\frac{R_s}{\eta_c} + R_L - R_H + \frac{R_H}{\eta_c} + 1\right) \qquad (20a)$$

$$= \frac{C_c}{\eta_c}\left(R_s + R_H + \eta_c\left(1 + R_L - R_H\right)\right) \qquad (20b)$$

This relationship can be used as the objective function for the design optimization of a sub-system (component) in a minimum weight system. The objective function can be simplified if certain relationships exist.

$$\text{IF} \quad R_s + R_H = 0 \qquad \text{OR} \qquad R_s + R_H <<< 1 + R_L - R_H \qquad (21a)$$

THEN $C_T \propto C_c$

or IF $\quad R_s + R_H >> 1 + R_L - R_H \qquad\qquad$ THEN $\quad C_T \propto \dfrac{C_c}{\eta_c} \qquad (21b)$

When little or no information is available on the specific weight ratios it is felt that the later simplified objective function gives a more suitable optimized sub-system design than the former simplified objective function.

Therefore, in the design optimization of a transformer or transformer-rectifier system as a sub-system in a system whose total weight is to be minimized, it is more desirable to use weight divided by efficiency rather than just weight as the design optimization objective function.

Figure 3-2

COMPARISON OF TWO MINIMUM WEIGHT
TRANSFORMER SYSTEM DESIGN OPTIMIZATION
OBJECTIVE FUNCTIONS (FIGURE OF MERIT)
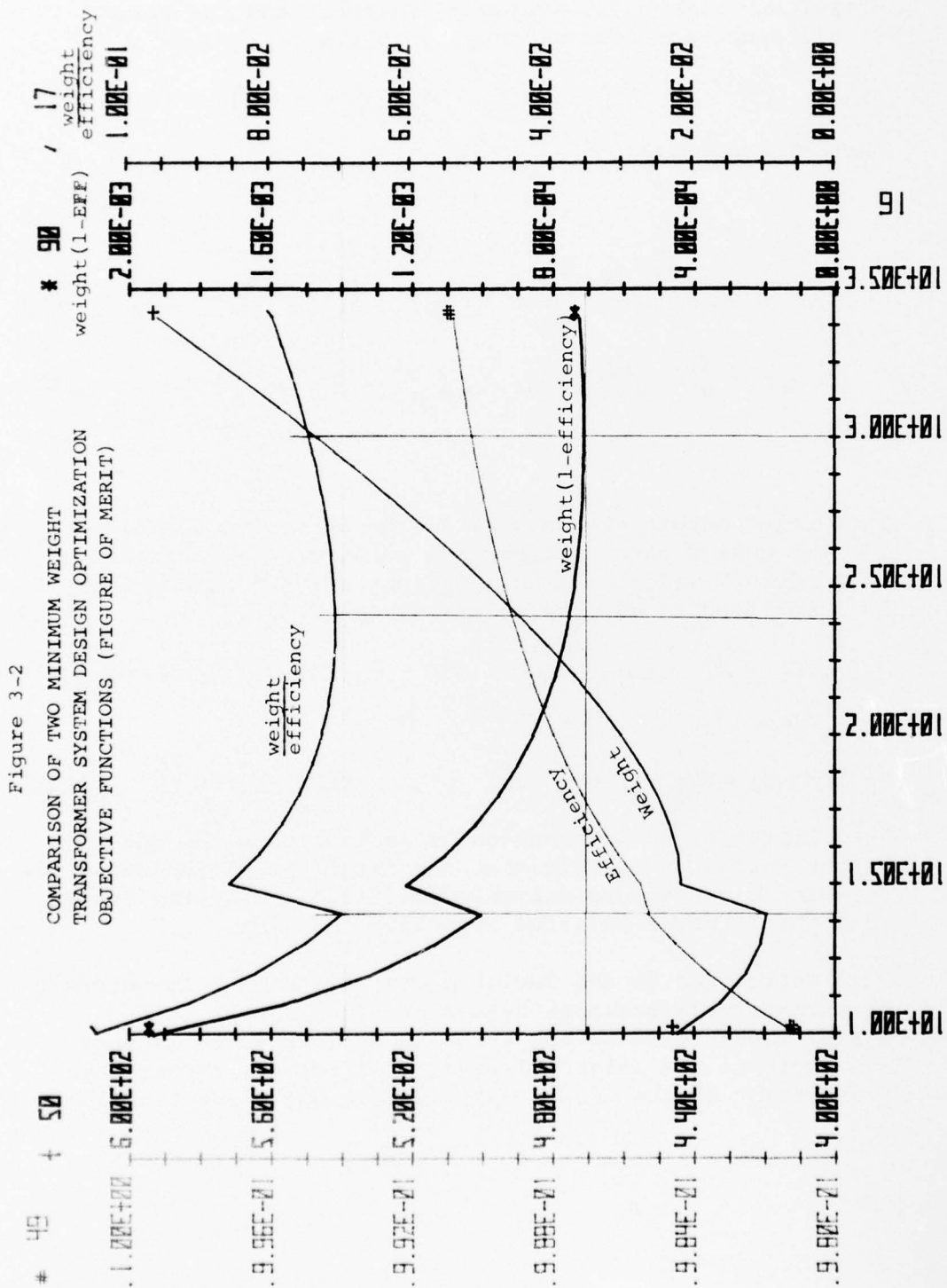
In general the preceeding statement says that it is desirable to maximize efficiency at the same time weight is being minimized. In maximizing efficiency, losses are being minimized, and therefore we should be able to restate our objective as the desire to minimize losses and weight. The two relationships are not identical as they possess different weightings as is indicated in Fig. 3-2. The latter, $W(1-\eta)$, favors higher efficiency and weight while the former $\frac{W}{\eta}$ favors lower efficiency and weight. The difference arises from the fact that as $(1-\eta)$ goes from 0 to 1; $\frac{1}{\eta}$ goes from 1 to ∞. As the system analysis shows $\frac{C}{\eta}$ to be the optimization function for minimizing total system weight, then a sub system optimized using the objective function $C(1-\eta)$ will not yield the desired results but rather one that favors higher efficiencies at the expence of higher total system weight.

3.1.4 Sample Run and Flow Chart

Listing 1 presents a sample run. A user flow chart is presented in Figure 3-3.

19

Figure 3-3   (continued)

A

?
LIST PARAMETER DEF.
AS READ IN FROM
INITIAL DATA SET

YES   NO

ENTER "Y"   ENTER "N"

?
CHANGE/ENTER
FIXED INDEPENDENT   YES   ENTER:
PARAMETER VALUE   PAR. #, VALUE

NO

ENTER: 0,0

?
ENTER OPTIMIZABLE   YES   ENTER: PAR. #,
PARAMETER DATA   INITIAL VALUE,
                                 INCREMENT,
NO   FINAL VALUE,
                                 # INCREMENTS
ENTER: 0,0,0,0,0

?
ENTER OPTIMIZATION   YES   ENTER: OBJECTIVE
FUNCTION DATA   FUNCT. PAR. #,
                                 MIN/MAX MULT.
NO

ENTER: 0,0

?   YES   ENTER: RANGED PAR. #,
ENTER MULTIPLE LISTED DESIGNS,   INITIAL VALUE,
INDEP. PAR. RANGE DATA   INCREMENT,
                                     FINAL VALUE,
NO   # INCREMENTS

B

20

Figure 3-3 (continued)

Listing 1

```
ASD COMPUTER CENTER INTERCOM 4.5
SYSTEM  CSA
DATE  11/05/76      TIME  11.42.37.

PLEASE LOGIN
LOGIN,P720483,    ,353

11/05/76   LOGGED IN AT  11.42.58.
           WITH USER-ID VO
           EQUIP/PORT 16/031
SCREEN,132

ATTACH,TAPE1,TDPD

 PF CYCLE NO. = 005
ATTACH,TDOP2

 PFN IS
 TDOP2
 PF CYCLE NO. = 002
TDOP2

N
```

NO.	CONSTANT INDEPENDENT PARAMETER VALUE
1	115.00
2	115.00
5	100000
7	.32400
8	.32400
9	.29800
10	.56500E-01
17	.85000
19	60.000
20	.55000E-01
22	75.000
23	125.00
24	.10000E-02
25	0.
26	0.
27	0.
28	1.0000
29	1.0000
31	.15300E-02
33	.50000
34	125.00
35	10.000
37	.11517E-08
38	1.3202
39	1.1129
46	2.0000
48	2.0000
87	0.
91	.78125
92	1.2500
101	.58440E-06

NO.	VALUE
101	.58440E-06
102	.58440E-06
105	.23720E-02
106	.23720E-02
109	22.000
110	22.000
112	2.0000
113	500.00
115	1.1000
120	1.0000
124	.25000E-01
125	.50000
126	0.
127	.47200E-02
154	0.
155	0.
156	2.0000
162	0.
165	1.0000
169	.62500
170	1.7500
174	125.00
175	175.00
181	1.0000
182	.50000
183	.25000
206	0.
207	0.
208	.50000E-01
209	100000
210	50000.
211	.20000E+06
224	.50000E-01
225	.50000E-01
233	97.000
234	97.000
235	126.00
245	0.
246	3.0000
247	527.00
248	.50000E-01
249	386.00
250	0.
260	110.00
262	.18300E-02
263	.69480E-04
264	.34700E-01
279	.50000E-01

Listing 1   (continued)

NO. , FIXED INDEPENDENT PARAMETER VALUES

ENTER 0,0 TO END FIXED DATA VALUE INPUT

1,10000

   1   10000.

2,265

   2   265.00

5,90000

   5   90000.

17,.8

  17   .80000

19,10000

  19   10000.

25,120

  25   120.00

28,.5

  28   .50000

33,.7

  33   .70000

35,10000

  35   10000.

46,1

  46   1.0000

48,10

  48   10.000

91,.11820

  91   .11820

92,1

  92   1.0000

99,4E-8

  99   .40000E-07

110,36

 110   36.000   91,1.125

208,.1

                     91   1.1250

 208   .10000   92,.5

245,900

                     92   .50000

 245   900.00   0,0

Listing 1 (continued)

```
PAR.#, INITIAL VALUE, INCREMENT, FINAL VALUE,#INCREMENTS
ENTER 0,0,0,0,0 TO END OPTIMIZABLE PARAMETER DATA INPUT

 O#   P#  INITIAL VALUE      INCREMENT    FINAL VALUE   NUMBER OF OPTIMIZ

46,1,1,3,0

  1   46    1.0000            1.0000       3.0000           0
48,2,2,22,0

  2   48    2.0000            2.0000       22.000           0
109,16,1,22,0

  3  109    16.000            1.0000       22.000           0
110,34,1,38,0

  4  110    34.000            1.0000       38.000           0
0,0,0,0,0

  5    0    0.                0.           0.               0
 INPUT OPTIMIZATION FUNCTION DATA :
 PARAMETER #, MIN.MAX.MULT.#
 ENTER 0,0 TO END INPUT OF OPTIMIZATION FUNCTION DATA!
90,1


OBJECTIVE FUNCTION PARAMETER NUMBER =   90 , MULTIPLYING FACTOR =  1.00

0,0


OBJECTIVE FUNCTION PARAMETER NUMBER =    0 , MULTIPLYING FACTOR =  0.

 INPUT VARIABLE INDEPENDENT PARAMETER RANGE DATA :
 PAR.#, INITIAL VALUE, INCREMENT, FINAL VALUE,#INCREMENTS
 ENTER 0,0,0,0,0 TO END PARAMETER RANGE DATA INPUT !

 R#   P#  INITIAL VALUE      INCREMENT    FINAL VALUE   NUMBER OF RANGED

0,0,0,0,0

  1    0    0.                0.           0.               0
 INPUT CONSTRAINED (BOUNDED) DEPENDENT PARAMETER DATA :
 PARAMETER # , BOUND VALUE , LIMIT TYPE
 ENTER 0,0,0 TO END CONSTRAINT VALUE DATA INPUT !

 C#   P#  BOUNDRY VALUE   LIMIT TYPE

42,1.75,-1

  1   42    1.7500         -1
43,1.75,-1

  2   43    1.7500         -1
0,0,0

  3    0    0.              0
 INPUT PARAMETER LISTING DATA :
 PARAMETER # ; ENTER 0 (ZERO) TO END LISTING DATA INPUT!

 D#   P#
```

24

```
1,
  1    0
```

Listing 1 (continued)

OPTIMAL POINT DESIGN #   1   11/05/76   11.59.46.

PAGE 1   OPTIMAL DESIGN 1   9.515 SECONDS   11/05/76

CONSTRAINED OPTIMAL DESIGN

```
 1 : AVG.DC.OUTPUT EMF,3-PHASE BRIDGE RECTIF  =    10000.       VOLTS,AVG.
 2 : PRIMARY LINE-LINE EMF                    =    285.00       VOLTS,RMS
 3 : PRIMARY CONDUCTOR RESISTIVITY,AVERAGE    =    .72302E-06   OHM-INCHES,AV
 4 : SECONDARY WINDING CONDUCTOR RESISTIVITY  =    .72302E-06   OHM-INCHES,AV
 5 : PEAK MAGNETIC INDUCTION DENSITY          =    90000.       LINES/SQ.IN.,
 6 : MINIMUM OPERATEINF FREQUENCY             =    5000.0       HERTZ,MIN.
 7 : PRIMARY WINDING CONDUCTOR DENSITY        =    .32400       POUNDS/CUBIC
 8 : SECONDARY WINDING CONDUCTOR DENSITY      =    .32400       POUNDS/CUBIC-
 9 : CORE DENSITY                             =    .29800       POUNDS/CUBIC-
10 : COOLANT DENSITY                          =    .56500E-01   POUNDS/CUBIC-
11 : PRIMARY WINDING CONDUCTOR COOLING RATE   =    67.086       WATTS/SQUARE-
12 : SECONDARY WINDING CONDUCTOR COOLING RATE =    7.3650       WATTS/SQUARE-
13 : CORE DISSIPATION RATE                    =    52.301       WATTS/POUND
14 : CORE LEG WIDTH                           =    1.5000       INCHES
15 : CORE LEG DEPTH                           =    .75000       INCHES
16 : NUMBER OF PRIMARY TURNS PER LAYER        =    17.261       TURNS/LAYER,P
17 : CORE STACKING FACTOR                     =    .80000       UNITS/UNITS
18 : PRIMARY SPACING BTWN TURNS               =    .14072E-02   INCHES
19 : MAXIMUM OPERATEING FREQUENCY             =    10000.       HERTZ,MAX.
20 : CORE INSULATION DENSITY (=.055)          =    .55800E-01   POUNDS/CUBIC
21 : SPACING BETWEEN TURNS IN SECONDARY LAYER =    .55520E-03   INCHES
22 : INITIAL CONDUCTOR TEMPERATURE            =    75.000       DEG.F.
23 : FINAL CONDUCTOR TEMPERATURE              =    125.00       DEG.F.
24 : EFFICIENCY CONVERGENCE CRITERION         =    .10000E-02   /UNIT
25 : ON TIME/MAJOR CYCLE                      =    120.00       SECONDS
26 : PRIMARY CONNECTION FACTOR ( 3 = DELRA )  =    0.           0=1-PHASE
27 : SE ONDARY CONNECTION FACTOF ( 1 = WYE )  =    0.
28 : PER UNIT FREQUENCY DROOP                 =    .50000
29 : RMS LOAD CURRENT WAVEFORM FACTOR         =    1.0000       AMPS/AMP
30 : NO. OF INTEERLEAVINGS(PRI-SEC.INTERFACES =    2.0000       (INTERLEAVING
31 : COOLING SPACING FACTOREVAPOR. COOLING)   =    .15306E-02   IN/(IN-WATT/S
32 : NUMBER OF CONVERGENCE ITTERATIONS        =    7.0000
33 : MINIMUM EFF ICIENCY                      =    .70000       /UNIT
34 : MAXIMUM CORE TEMPERATURE                 =    125.00       DEGREES FAREN
35 : OUTPUT POWER,BRIDGE RECTIFIER            =    10000.       WATTS , DC
36 : CORE IRON WEIGHT                         =    1.7918       POUNDS
37 : CORE LOSS COEFFIC IENT                   =    .11517E-08
38 : CORE LOSS BM EXPONENT                    =    1.3262
39 : CORE LOSS FREQUENCY EXPLNENT             =    1.1129
40 : PRIMARY       DIAMETER,CONDUCTOR         =    .28284E-01   INCHES,PRI.
41 : SECONDARY     DIAMETER,CONDUCTOR         =    .49999E-02   INCHES,SEC.
42 : WINDOW WIDTH                             =    .82539       INCHES
43 : WINDOW HEIGHT                            =    1.0151       INCHES
44 : NUMBER OF PRIMARY TURNS PER COIL         =    17.261       TURNS/COIL,PR
45 : NUMBER OF SECONDARY TURNS PER COIL       =    696.61       TURNS/COIL,SE
46 : NUMBER OF PRIMARY LAYERS PER COIL        =    1.0000       LAYERS/COIL,P
47 : NUMBER OF SECONDARY TURNS PER LAYER      =    87.076       TURNS/LAYER,S
48 : NUMBER OF SECONDARY LAYERS PER COIL      =    8.0000       LAYERS/COIL,S
49 : COMPUTED EFFICIENCY                      =    .95837       /UNIT
50 : TOTAL WEIGHT,TRANS:CORE,COILS,COOLANT    =    2.4554       POUNDS
```

25

Listing 1 (continued)

PAGE 2 OPTIMAL DESIGN 1 9.515 SECONDS 11/05/76

CONSTRAINED OPTIMAL DESIGN

51 :	REGULATION	=	.36220E-01 /UNIT
52 :	INPUT LINE CURRENT	=	40.606 AMPERES,RMS
53 :	RECTIFIED OUTPUT CURRENT	=	1.0000 AMPERES,DC,AV
54 :	TOTAL INPUT POWER	=	11573. VOLT-AMPERES,
55 :	PRIMARY WINDING CURRENT	=	40.606 AMPERES,RMS,P
56 :	PRIMARY CURRENT DENSITY,RMS	=	65176. AMPERES/SQ.IN
57 :	SECONDARY CURRENT DENSITY,RMS	=	51095. AMPERES/SQ.IN
58 :	PRIMARY CONDUCTOR CROSSECTIONAL AREA	=	.62831E-03 SQUARE-INCHES
59 :	SECONDARY CONDUCTOR CROSS-SECTIONAL AREA	=	.19634E-04 SQUARE-INCHES
60 :	MAGNETIC INDUCTION IN CORE	=	81000. LINES
61 :	PER UNIT RESISTANCE	=	.11655 OHMS/OHM
62 :	TOTAL PRIMARY-TO-SECONDARY SPACING	=	.27869 INCHES
63 :	WINDING DEPTH(PRI.+SEC.+SPACING)	=	.54157 INCHES
64 :	PRIMARY LENGTH PER COIL(MEAN)	=	114.11 INCHES/COIL,P
65 :	SECONDARY LENGTH PER COIL(MEAN)	=	4605.5 INCHES/COIL,S
66 :	PRIMARY RESISTANCE PER COIL	=	.13243 OHMS/COIL,PRI
67 :	SECONDARY RESISTANCE PER COIL	=	170.14 OHMS/COIL,SEC
68 :	DISSIPATION PER COIL(PRI.+SEC.)	=	388.50 WATTS/COIL
69 :	TOTAL WIRE VOLUME(PRI.+SEC.)	=	.16212 CUBIC-INCHES
70 :	TOTAL WIRE WEIGHT(PRI.+SEC.)	=	.52528E-01 POUNDS
71 :	CORE VOLUME , PHYSICAL	=	7.5161 CUBIC-INCHES
72 :	CORE WEIGHT , TOTAL	=	1.8745 POUNDS
73 :	CORE DISSIPATION,EDDY-CURRENT+HYSTERESIS	=	93.716 WATTS,CORE-TO
74 :	TOTAL DISSIPATION(CORE+COILS)	=	482.22 WATTS,TRANS-T
75 :	PRIMARY CONDUCTOR VOLUME	=	.71699E-01 CUBIC-INCHES,
76 :	SECONDARY WIRE VOLUME	=	.90425E-01 CUBIC-INCHES,
77 :	TANK INTERNAL VOLUME	=	28.095 CUBIC-INCHES,
78 :	COOLANT VOLUME	=	9.3507 CUBIC-INCHES,
79 :	COOLANT WEIGHT	=	.52832 POUNDS,COOLAN
80 :	PRIMARY EMF PER TURN	=	16.512 VOLTS/TURN,PR
81 :	SECONDARY EMF PER TURN	=	15.934 VOLTS/TURN,SE
82 :	BARE WIRE CROSSECTIONAL AREA	(=	0. QUARE INCHES
83 :	INSULATED WIRE CROSSECTIONAL AREA	(=	0. QUARE INCHES
84 :	LEAKAGE INDUCTANCE REFERED TO SECONDARY	=	.92227E-02 HENRIES
85 :	LEAKAGE REACTANCE REFERED TO SECONDARY	=	579.48 OHMS
86 :	ASSUMED INITIAL TRANSFORMER DESIGN EFFIC	=	.19688 /UNIT
87 :	ABSOLUTE MINIMUM SPACING	=	0. INCHES
88 :	PER UNIT REACTANCE	=	.17384 OHMS/OHM
89 :	PER UNIT IMPEDANCE	=	.20930 OHMS/OHM
90 :	EFFICIENCY PER POUND PER KILLOWATT OUT	=	.13993E-01 1/LBS+KILLOWA
91 :	CORE LEG CROSS-SECTIONAL AREA	=	1.1250 SQUARE-INCHES
92 :	CORE LEG ASPECT RATIO (DEPTH/WIDTH)	=	.50000 INCHES/INCH
93 :	CASE INTERNAL HEIGHT	=	2.5151 INCHES
94 :	CASE DEPTH	=	2.4018 INCHES
95 :	CASE WIDTH	=	4.6508 INCHES
96 :	SECONDARY LINE CURRENT	=	1.0000 AMPERES,RMS/L
97 :	SECONDARY WINDING CURRENT	=	1.0000 AMPERE,RMS/WI
98 :	SECONDARY LINE-TO-LINE EMF	=	11100. VOLTS,RMS,SEC
99 :	DRIVING WAVEFORM FACTOR (4E-8*SO+4.44*SI)	=	.40000E-07 N
100 :	NO LOAD SECONDARY LINE-TO-LINE EMF	=	11502. VOLTS,RMS,SEC

26

Listing 1 (continued)

CONSTRAINED OPTIMAL DESIGN

```
101 : ZERO DEGREE PRIMARY CONDUCTOR RESISTIVIT =      .58440E-06 OHM-INCHES@0.
102 : ZERO DEGREE SECONDARY CONDUCTOR RESISTIV =      .58440E-06 OHM-INCHES@0.
103 : PRIMARY CONDUCTOR TEMPERATURE,AVERAGE    =      100.00     DEGREES-F.,AV
104 : SECONDARY CONDUCTOR TEMPERATURE,AVERAGE  =      100.00     DEGREES-F.,AV
105 : PRIMARY CONDUCTOR TEMPERATURE COEFFICIEN =      .23720E-02 UNITS/DEGREE-
106 : SEC.CON.TEMPERATURE COEFF.OF RESISTIVITY =      .23720E-02 UNITS/DEGREE-
107 : PRIMARY AC-TO-DC RESISTANCE RATIO        =      1.0085     OHMS/OHM
108 : SECONDARY AC-TO-DC RESISTANCE RATIO      =      1.0032     OHMS/OHM
109 : PRIMARY WIRE GAUGE / NO. LITZ WIRE       =      21.000     STRANDS
110 : SECONDARY WIRE GAUGE/NO.LITZ WIRE        =      36.000     STRANDS
111 : NUMBER OF RECTIFIER DEVICES PER STACK    =      43.521     RECTIFIERS/ST
112 : RECTIFIER BREAKDOWN FACTOR               =      2.0000     VOLTS/VOLT
113 : RECTIFIER PEAK REVERSE EMF               =      500.00     VOLTS,PEAK
114 : SECONDARY EMF PER WINDING                =      11100.     VOLTS-WINDING
115 : FORWARD EMF DROP PER RECTIVIER ELEMENT   =      1.1000     VOLTS-ELEMENT
116 : SECONDARY VA                             =      11100.     VOLTS-AMPERES
117 : PRIMARY HEIGHT                           =      .51249     INCHES,PRI.
118 : SECONDARY HEIGHT                         =      .48372     INCHES,SEC.
119 : CORE COOLING RATE,STEADY STATE           =      4.6758     WATTS/SQ.IN.
120 : SERIES FACTOR , INSULATION               =      1.0000     VOLTS/VOLT
121 : MINIMUM RELATIVE SPACING FACTOR          =      0.         INCHES/INCH
122 : ENCLOSURE HEATING RATE                   =      0.         WATTS/SQ.IN.
123 : SECONDARY EMF PER LAYER                  =      1437.8     VOLTS/LAYER,S
124 : MINIMUM COOLING SPACE                    =      .25000E-01 NINCHES
125 : MAXIMUM COOLING SPACE                    =      .50000     NINCHES
126 : MAXIMUM OPERATING TILT ANGLE             =      0.         RADIANS
127 : RATIO COOLANT VAPOR/LIQUID DENSITY       =      .47200E-02 (#/CU.IN.)/(#
128 : PRIMARY-TO-SECONDARY HORIZONTAL SPACING  =      .15665     INCHES
129 : EMF SEC.L-L + EMF PRI.L-L                =      0.         VOLTS
130 : SPACING,HOR.INSIDE LAYER-TO-CORE INSIDE  =      .16488     INCHES
131 : PPACING,HOR.INNER LAYER-TO-CORE OUTSIDE  =      .16540     INCHES
132 : SPACING,HRR.OUTER LAYER-TO-ENCLOSURE     =      .11894     INCHES
133 : SPACING,HORIZONTAL,SECONDARY-TO-SEC.LAYE =      .32534E-01 INCHES
134 : SPACING,HOR.OUTER-TO-OUTER LAYER         =      .12286     INCHES
135 : SPACING,VERTICAL,TOP SECONDARY-TO-CORE   =      .25501     INCHES
136 : SPACING,VERT.BOTTOM SECONDARY-TO-CORE    =      .76380E-01 INCHES
137 : SPACING,HORIZONTAL,SECONDARY-TO-PRIMARY  =      .12144     INCHES
138 : SPACING,VERTICAL,TOP PRIMARY-TO-CORE     =      .24063     INCHES
139 : SPACING,VER.BOTTOM PRIMARY-TO-CORE       =      .61993E-01 INCHES
140 : PRIMARY WINDING EMF                      =      285.00     VOLTS,RMS,PRI
141 : SPACING,HORIZONTAL,PRIMARY-TO-PRIMARY LA =      .52363E-01 INCHES
142 : PRIMARY CONDUCTOR LOSS RATE              =      219.36     WATTS
143 : SECONDARY CONDUCTOR LOSS RATE PER COIL   =      170.14     WATTS
144 : SECONDARY IMPEDANCE                      =      603.94     OHMS,SEC.
145 : NECESSARY WINDOW HEIGHT FOR PRIMARY      =      .75293     INCHES,PRI.
146 : NECESSARY WINDOW HEIGHT FOR SECONDARY    =      .66958     INCHES,SEC.
147 : NUMBER OF SECONDARY GROUPS               =      2.0000     GROUPS/SEC.
148 : MINIMUM NUMBER OF LAYERS IN A SECONDARY  =      4.0000     LAYER/GROUP,M
149 : MAXIMUM NO.OF LAYERS PER SECONDARY GROUP =      5.0000     LAYER/GROUP,M
150 : NUMBER OF SEC.GROUPS WITH MIN.NO.LAYERS  =      2.0000     GROUPS/SEC.,M
```

Listing 1 (continued)

PAGE 4   OPTIMAL DESIGN 1   9.515 SECONDS   11/05/76

CONSTRAINED OPTIMAL DESIGN

```
151 : NUMBER OF SEC.GROUPS WITH MAX.NO.LAYERS  =      0.         GROUPS/SEC.,M
152 : MEAN COIL PERIMETER                      =      6.6113     INCHES
153 : EFFECTIVE CORE COOLING SURFACE AREA      =     16.634      SQUARE-INCHES
154 : CORE-TO-CASE HEAD SPACE, TOTAL           =       .99063    INCHES
155 : SPACING,HORIZONTAL FOR SUPPORT STRUCTURE =      0.         INCHES
156 : EMF WINDING BREAKDOWN FACTOR             =      2.0000     VOLTS/VOLT
157 : NUMBER OF PRIMARY GROUPS                 =      1.0000     GROUPS/PRI.
158 : MINIMUM NUMBER OF LAYERS PER PRIMARY GRO =      1.0000     LAYER/GROUP,M
159 : MAXIMUM NUMBER OF LAYERS PER PRI.GROUP   =      2.0000     LAYER/GROUP,M
160 : NUMBER OF MINIMUM LAYER PRIMARY GROUPS   =      1.0000     GROUPS/PRI,MI
161 : NUMBER OF MAXIMUM LAYER PRIMARY GROUPS   =      0.         GROUPS/PRI.,M
162 : WIRE GAUGE NUMBER(0=SOLID)            ( =      0.
163 : BARE WIRE DIAMETER                    ( =      0.         INCHES
164 : INSULATED WIRE DIAMETER               ( =      0.         INCHES
165 : DUTY FACTOR                              =      1.0000     SECONDS/SECON
166 : ENCLOSURE WEIGHT                         =      0.         POUNDS
167 : AIR FLOW PATH WIDTH                      =      0.         INCHES
168 : AIR FLOW PATH DEPTH                      =      0.         INCHES
169 : TUBE DIAMETER                            =       .62500    INCHES
170 : TUBESPACING(WIDTH&DEPTH)                 =      1.7500     INCHES
171 : NUMBER OF ROWS DEEP                      =      0.         ROWS
172 : NUMBER OF ROWS WIDE                      =      0.         ROW
173 : AIR MASS FLOW RATE                       =      0.         LBS/SEC-SQ.IN
174 : AMBIANT AIR TEMPERATURE                  =    125.00       DEG.FARENHEIG
175 : AVERAGE COOLANT TEMPERATURE              =    175.00       DEGREES FAREN
176 : AIR HEAT TRANSFER COEFFICIENT            =      0.         JOUL/SEC/SQ.I
177 : HEAT EXCHANGER SURFACE AREA TO AIR       =      0.         SQUARE INCHES
178 : FAN DIAMETER                             =      0.         INCHES
179 : WEIGHT TRANSFORMER + HEAT EXCHANGER      =      0.         INCHES
180 : VOLUME TRANSFORMER + HEAT EXCHANGER      =      0.         CUBIC INCHES
181 : VOLUME HEAT EXCHANGER LESS FAN           =      1.0000     CUBIC INCHES
182 : COOLANT PRESURE DROP O.F. EXPONENT       =       .50000
183 : COOLANT FLOW RATE O.F. EXPONENT          =       .25000
184 : INITIAL PRI.COND.RESISTIVITY            =       .68836E-06 OHM-INCHES
185 : INITIAL SEC.COND.RESISTIVITY            =       .68836E-06 OHM-INCHES
186 : INITIAL PRI.COND.RY.TEMP.COEFFICIENT    =       .20138E-02 /DEGFWTO
187 : INITIAL SEC.COND.RESISTIVITY TEMP.COEFF. =      .20138E-02 /DEG.F.RT O
188 : HEAT EXCHANGER SURFACE AREA TO INSIDE CO =      0.         SQUARE INCHES
189 : HEAT EXCHANGER VAPOR CONDENSATION COEFFI =      0.         JOUL/SEC/SQ.I
190 : BLOWER HORSE POWER                       =      0.         WATTS
191 : TUBE TEMPERATURE                         =      0.         DEGREES FEMEN
192 : HEAT EXCHANGER HEIGHT                    =      0.         INCHES
193 : PRESSURE DROP                            =      0.         INCHES/COOLAN
194 : AIR VELOCITY                             =      0.         INCHES/SEC
195 : CFM                                      =      0.         CUBIC-FEET/MI
196 : BLOWER WEITHT                            =      0.         POUNDS
197 : FIN TUBE WEIGHT                          =      0.         POUNDS
198 : HEAT EXCHANGER WEIGHT                    =      0.         POUNDS
199 : TRANSFORMER SYSTEM WEIGHT               =       0.         POUNDS
200 : SYSTEM OBJECTIVE FUNCTION               =        .77183E-03 EFF/WT/COMRT
```

28

Listing 1   (continued)

CONSTRAINED OPTIMAL DESIGN

```
201 : CONE LAMINATION EDGE SURFACE AREA         =      0.          SQ.IN.
202 : CORE LAMINATION FACE SURFACE AREA         =      0.          SQ.IN.
203 : CORE LAMINATION EDGE COOL RATE            =      0.          WATTS/SQ.IN.
204 : CORE LAMINATION FACE COOLING RATE         =      0.          WATTS/SQ.IN.
205 : CORE LAMINATION EDGE/FACE COOL RATE RATI  =      0.
206 : PRIMARY CONDUCTOR INSULATION THICKNESS    =      0.          INCHES
207 : SECONDARY CONDUCTOR INSULATION THICKNESS  =      0.          INCHES
208 : CON SURFACE INSULATION THICKNESS          =      .10000      INCHES
209 : CONDUCTOR AND CONE SUR. INSU. DIEL. STRE  =      100000      KV/IN.
210 : COOLING PASSAGE DIELECTRIC STRENGTH       =      50000.      KV/IN.
211 : INSU.BARRIER DIELECTRIC STRENGTH          =      .20000E+06  KV/IN.
212 : INN VERT. CONE FACE COOL SPACE HORI. THK  =      0.          INCHES
213 : OUT VERT. CONEFACE COOL. SPACE HOR. THK   =      .68602E-03  INCHES
214 : INN HOR. CONE FACE COOL SPACE VERT THICK  =      0.          INCHES
215 : COIL FORM INNER FACE THICKNESS            =      .64882E-01  INCHES
216 : COIL FORM OUTER FACE THICKNESS            =      .64710E-01  INCHES
217 : COIL FORM UPPER FACE THICKNESS            =      .13195E-02  INCHES
218 : COIL FORM LOWER FACE THICKNESS            =      .60864E-01  INCHES
219 : SEC-SEC LAYER INSU. BARRIER THICKNESS     =      .27125E-01  INCHES
220 : SEC-PRI LAYER INSU. BARRIER THICKNESS     =      .11603      INCHES
221 : PRI-PRI LAYER INSU. BARRIER THICKNESS     =      0.          INCHES
222 : OUT LAYER-ENCLO INSU BARRIER THICKNESS    =      .11353      INCHES
223 : OUT-OUT LAY INSU.BARRIER THICKNESS        =      .11204      INCHES
224 : TOTAL COOL SPACE THICK FOR ONE SEC LAYER  =      .54084E-02  INCHES
225 : TOTAL COOL SPACE THICK FOR ONE PRI LAYER  =      .52363E-01  INCHES
226 : COOL SPACE REQUIRED AT TOP OF PRI LAYER   =      .23931      INCHES
227 : COOL SPACE REQUIRED AT TOP OF SEC LAYER   =      .25369      INCHES
228 : COOL SPACE REQUIRED AT BOT OF PRI LAYER   =      .11295E-02  INCHES
229 : COOL SPACE REQUIRED ATBOT OF SEC LAYER    =      .15516E-01  INCHES
230 : INN SPACE BTWN UP AND LOW COIL FORM FACE  =      .75293      INCHES
231 : OUT SPACE BTWN UP AND LOW COIL FORM FACE  =      .81511      INCHES
232 : PRI-SEC.WIND.LAYER INSULATING BARIER THI  =      .10429      INCHES
233 : PRI.WIND.COND.SPECIFIC HEAT               =      97.000      JOULES/LB/DEG
234 : SEC. WIND. COND. SPECIFIC HEAT            =      97.000      JOULES/LB/DEG
235 : CORE SPECIFIC HEAT                        =      125.00      JOULES/LB/DEG
236 : PRI.WIND.COND.ON TRANSIENT COOLING RETE   =      66.780      WATTS/SQ.IN
237 : SEC. WIND. COND. ON TRANSIENT COOLING RA  =      7.3079      WATTS/SQ.IN
238 : CORE ON TIME TRANSIENT COOLING RATE       =      -1.1911     WATTS/SQ.IN
239 : PRI.WIND.COND.OFF TIME TRANS.COOLING RAT  =      .40716E-01  WATTS/SQ.IN
240 : SEC.WIND.COND.OFF TIME TRANS.COOLING RAT  =      .76178E-02  WATTS/SQ.IN
241 : CORE OFF TIME TRANSIENT COOLING RATE      =      .70225      WATTS/SQ.IN
242 : RATIO PRI.COND.VOL.TO COOLING SURFACE AR  =      .23319E-01  CU.IN/SQ.IN
243 : RATIO SEC.COND.VOL.TO COOLING SURFACE AR  =      .43630E-02  CU.IN/SQ.IN
244 : RATIO CORE VOLUME TO COOLING SURFACE ARE  =      0.          CU.IN/SQ.IN
245 : MAJOR CYCLE OFF TIME                      =      900.00      SECONDS
246 : COOLANT PRESSURE DROP ACROSS WINDINGS     =      3.0000      LBS/SQ.IN
247 : COOLANT SPECIFIC HEAT                     =      527.00      JOULES/LB/DEG
248 : PRESSURE DROP FRICTION FACTOR             =      .50000E-01
249 : GRAVITATIONAL CONSTANT = 386              =      386.00      INCHES/SEC/S
250 : CONDUCTION OVERLAP ANGLE                  =      0.          RADIANS
```

Listing 1 (continued)

PAGE 6   OPTIMAL DESIGN 1   9.515 SECONDS   11/05/76

CONSTRAINED OPTIMAL DESIGN

```
251 : PRIMARY WINDING COOLANT VELOCITY          =      0.          INCHES/SEC
252 : SECONDARY WINDING CIOLANT VELOCITY        =      0.          INCHES/SEC
253 : CORE COOLANT VELOCITY                     =      0.          INCHES/SEC
254 : RRIMARY WIND.COOLANT MASS FLOW RATE       =      0.          NLBS/SEC/IN
255 : SECONDARY WIND.COOLANT MASS FLOW RATE     =      0.          LBS/SEC/IN
256 : CORE COOLANT MASS FLOW RATE               =      0.          LBS/SEC/IN
257 : FRIMARY WIND.COOLANT TEMPERATURE RISE     =      0.          DEG.F
258 : SECONDARY WIND.COOLANT TEMPERATURE RISE   =      0.          DEG.F
259 : CORE COOLANT TEMPERATURE RISE             =      0.          DEG.F
260 : INCOMMING COOLANT TEMPERATURE             =    110.00        DEG.F
261 : OUTGOING COOLANT TEMPERATURE              =      0.          DEG.F
262 : COOLANT THERMAL CONDUCTIVITY              =    .18300E-02    JOULES/SEC/SQ
363 : COOLANT VISCOSITY AT SURFACE              =    .69400E-04    JLBS/IN/SEC
264 : BULK COOLANT VISCOSITY                    =    .34700E-03    JLBS/IN/SEC
265 : PRI.WIND-COOL.HEAT TRANSFER COEFFICIENT   =      0.          JOULES/SEC/SQ
266 : SEC.WIND-COOL.HEAT TRANSFER COEFFICIENT   =      0.          JOULE/SEC/SQ.
267 : CORE-COOLANT HEAT TEANSFER COEFFICIENT    =      0.          JOULE/SEC/SQ.
268 : NECESSARY PRIMARY WINDING COOLING RATE    =     66.780       WATTS/SQ.IN
269 : NECESSARY SECONDARY WINDING CONDUCTOR CO  =      7.3079      OATTS/SQ.IN
270 : NECESSARY CORE COOLING RATE               =      .55009      WATTS/SQ.IN
271 : PRIMARY WIND.COOLANT MASS FLOW RATE       =      0.          LBS/SEC
272 : SECONDARY WINDING COOLANT MASS FLOW RATE  =      0.          LBS/SEC
273 : CORE COOLANT MASS FLOW RATE               =      0.          LBS/SEC
274 : TOTAL COOLANT MASS FLOW RATE              =      0.          LBS/SEC
275 : EFFORT * FLOW - PRODUCT                   =      0.
276 : PRIMARY COOLANT FLOW RENALDS NUMBER       =      0.
277 : SECONDARY COOLANT FLOW RENALDS NUMBER     =      0.
278 : CORE LEG COOLANT FLOW RENALDS NUMBER      =      0.
279 : FORCED COOLING CHANEL SPACING INCREMENT   =    .50000E-02
```

STOP NORMAL JOB EXECUTION COMPLETED

   11.222 CP SECONDS EXECUTION TIME
LOGOUT

CPA   12.250 SEC.   4.407 ADJ.
CRUS   9.258
CONNECT TIME   0 HRS.   34 MIN.
 11/05/76 LOGGED OUT AT 12.16.33.

3.1.5 Recommendations for Improvements to Present Program

There are two general areas in which the present program can be improved. They are: 1, the transformer design procedure, and 2, the central and optimization procedure. Improvements in the transformer design procedure to incorporate appropriate physical and thermo-electro-magnetic relationships to design transformers having structures not presently incorporated in the procedure (i.e., PIE windings, etc.) and allow for a more general selection of independent and dependent parameters by the user are recommended. Also recommended are improvements to the control data I/O, and optimization procedures to increase user and program efficiency and ease of utilization and reduce execution times.

3.2 10 KW Transformer Development

3.2.1 Design of Original 10 KW Unit

Numerous parametric sensitivity analyses were conducted to derive the design of a 10 KHz, 10 KVA inverter transformer, with both ferrite and Orthonol cores. Table I is a comparative listing of the parameters for optimized transformers with ferrite and Orthonol cores. Figures 3-4 & 3-5 are sketches of these optimized transformers.

Significant comparisons are: (1) Weight (K50); 0.909 lbs Orthonol core vs 2.47 ferrite core; (2) efficiency (K49); 93.6% Orthonol core vs 81.0% ferrite core; and (3) total volume (K77); 12.92 cu.in. Orthonol core vs 31.24 cu.in. ferrite core. The weights and volumes do not include any auxiliary heat transfer apparatus. If this were included, the Orthonol core transformer would show a further advantage in weight, due to its higher efficiency.

It is interesting to note that the core dissipation (K73) is lower for the ferrite (8.78 watts) than for the Orthonol (23.3 watts), but that this advantage is insignificant compared to the copper losses (K68) of 2335 watts for the ferrite and 659 watts for the Orthonol.

31

TABLE 1

10KHZ

K		ORTHONAL	FERRITE
1	OUTPUT VOLTAGE,VOUT	10000	10000
2	INPUT VOLTAGE,VIN	285	285
3	PRIMARY RESISTIVITY,PP,OHM-IN	6.78E-7	6.78E-7
4	SECONDARY RESISTIVITY,PS,OHM-IN	6.78E-7	6.78E-7
5	PEAK FLUX DENSITY,BMAX,LINES/SQ.IN.	96775	16130
6	FREQUENCY,HZ	10000	10000
7	PRIMARY WIRE DENSITY,LBS/CU.IN.	.324	.324
8	SECONDARY WIRE DENSITY,LBS/CU.IN.	.324	.324
9	CORE DENSITY,LBS/CU.IN.	.296	.276
10	COOLANT DENSITY,LBS/CU.IN.	.0505	.0505
11	PRIMARY HEATING RATE,HRP,WATTS/SQ.IN.	11.8	14.5
12	SECONDARY HEATING RATE,HRS,WATTS/SQ.IN.	2.2	3.5
13	CORE DISSIPATION RATE,PC,WATTS/LB.	130	11
14	CORE LEG WIDTH,A,IN.	.316	.548
15	CORE LEG DEPTH,B,IN.	.316	.548
16	PRIMARY TURNS/LAYER,NDP	36.2	69.8
17	COUPLING COEFFICIENT,CC	.999	.999
18	PRIMARY SPACE BETWEEN TURNS,S1P,IN.	.001	.001
19	PRIMARY SPACE BETWEEN LAYERS,S2P,IN.	.05	.052
20	PRIMARY-TO-CORE END SPACE(VERT),S3P,IN.	.065	.168
21	SECONDARY SPACE BETWEEN TURNS,S1S,IN.	.001	.001
22	SECONDARY SPACE BETWEEN LAYERS,S2S,IN.	.05	.05
23	SECONDARY-TO-CORE END SPACE(VERT),S3S,IN.	.133	.241
24	EFFICIENCY INCR (MAX.ALL.ERROR),DECIMAL	.0001	.0001
25	COOLANT HEAT OF VAPORIZATION,HFG,BTU/LB	63.12	63.12
26	PRIMARY CONNECTION FACTOR	1	1
27	SECONDARY CONNECTION FACTOR	1	1
28	PRIMARY WIRE THCK(RECT.WIRE ONLY)	-	-
29	SECONDARY WIRE THCK(RECT.WIRE ONLY)	-	-
30	NUMBER OF INTERLEAVINGS	4	4
31	COOLING SPACING FACTOR,IN./(WATTS/SQ.IN.)	1.53E-3	1.53E-3
32	PRIMARY-TO-CORE END SPACE(HORIZ),SPC,IN.	.05	.05
33	PRIMARY-TO-SECONDARY SPACE,SPS,IN.	.05	.05
34	SEC-TO-SEC SPACE(BETWEEN COILS),SSS,IN.	.05	.05
35	OUTPUT POWER,WATTS	10000	10000
36	AIR GAP LENGTH,IN.	.001	.001
37	RELATIVE PERMEABILITY	15000	5000
38	EQUIVALENT CORE LENGTH,OUTER LEG,IN.	-	-
39	EQUIVALENT CORE LENGTH,INNER LEG,IN.	-	-
40	PRIMARY WIRE DIAMETER,DIAP,IN.	.032(20)	.032(20)
41	SECONDARY WIRE DIAMETER,DIAS,IN.	.005(36)	.004(38)
42	WINDOW WIDTH,E,IN.	1.039	1.032
43	WINDOW HEIGHT,D,IN.	1.359	2.692
44	NUMBER OF PRIMARY TURNS/COIL,NP	72.38	139.64
45	NUMBER OF SECONDARY TURNS/COIL,NS	2709.9	6049.4
46	NUMBER OF PRIMARY LAYERS/COIL,NPL	2	2
47	NUMBER OF SECONDARY TURNS/LAYER,NSD	182.2	419.9
48	NUMBER OF SECONDARY LAYERS/COIL,NSL	15	15
49	EFFICIENCY	93.6	81.0

TABLE 1, CONT

K		ORTHONAL	FERRITE
50	TOTAL WEIGHT,WTOT,LBS.	.909	2.47
51	REGULATION,REG	93.7	81.0
52	COOLANT FLOW RATE,LBS/SEC.	.0102	.0352
53	OUTPUT CURRENT,IOUT,AMPS	1	1
54	INPUT POWER,PIN,WATTS	10681.4	12342.3
55	INPUT CURRENT,IIN,AMPS	37.48	43.31
56	PRIMARY CURRENT DENSITY,JP,AMPS/SQ.IN.	46656	51414
57	SECONDARY CURRENT DENSITY,JS,AMPS/SQ.IN.	50957	69995
58	PRIMARY WIRE CSA,AP,SQ.IN.	8.03E-4	8.42E-4
59	SECONDARY WIRE CSA,AS,SQ.IN.	.196E-4	.143E-4
60	FLUX IN CORE,LINES	9674.8	4838.7
61	PRIMARY DEPTH,DP,IN.	.114	.118
62	SECONDARY DEPTH,DS,IN.	.775	.764
63	TOTAL WINDING DEPTH,DSP,IN.	1.039	1.032
64	PRIMARY LENGTH/COIL,LP,IN.	153.5	427.5
65	SECONDARY LENGTH/COIL,LS,IN.	13800.5	36188.5
66	PRIMARY RESISTANCE/COIL,RP,OHMS	.13	.34
67	SECONDARY RESISTANCE/COIL,RS,OHMS	476.8	1696.9
68	DISSIPATION/COIL,PJ,WATTS	658.8	2334.8
69	TOTAL WIRE VOLUME,VW,CU.IN.	.394	.877
70	TOTAL WIRE WEIGHT,WW,LBS.	.128	.284
71	CORE VOLUME,VC,CU.IN.	.606	2.891
72	CORE WEIGHT,WC,LBS.	.179	.798
73	CORE DISSIPATION,PC,WATTS	23.3	8.78
74	TOTAL DISSIPATION,PL,WATTS	682.1	2343.6
75	PRIMARY WIRE VOLUME/COIL,VWP,CU.IN.	.123	.360
76	SECONDARY WIRE VOLUME/COIL,VWS,CU.IN.	.270	.517
77	TANK VOLUME,VT,CU.IN.	12.92	31.24
78	COOLANT VOLUME,VF,CU.IN.	11.92	27.47
79	COOLANT WEIGHT,WF,LBS	.602	1.39
80	PRIMARY VOLTS/TURN	3.94	2.04
81	SECONDARY VOLTS/TURN	3.69	1.65
82	PRIMARY SELF INDUCTANCE,CENTER LEG,HENRYS	13.9E-3	95.3E-3
83	PRIMARY SELF INDUCTANCE,OUTER LEG,HENRYS	-	-
84	SEC SELF INDUCTANCE,CENTER LEG,HENRYS	19.5	178.8
85	SEC SELF INDUCTANCE,OUTER LEG,HENRYS	-	-
86	INCREMENTAL EFFICIENCY,DECIMAL	-	-
87	MINIMUM SPACING,IN.	.05	.05
88	LEAKAGE INDUCTANCE REL TO SECONDARY,HENRYS	.015E-3	.037E-3
89	LEAKAGE INDUCTANCE REL TO PRIMARY,HENRYS	24.1E-3	73.9E-3
90	FIGURE OF MERIT	-	-
91	CORE CSA,SQ.IN.	0.1	0.3
92	CORE ASPECT RATIO=DEPTH/WIDTH	1	1
93	TANK WIDTH,IN.	2.71	3.16
94	TANK DEPTH,IN.	2.39	2.61
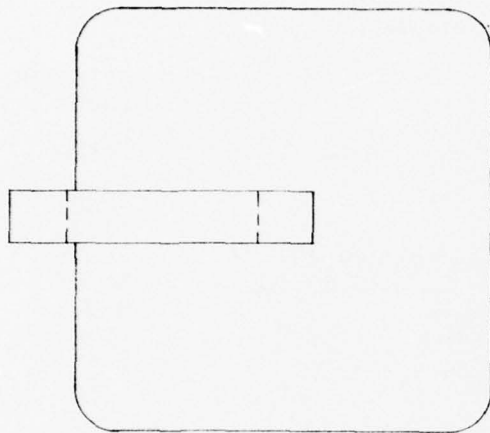
SCALE : FULL
SP. WT. = 0.09 LB/KVA
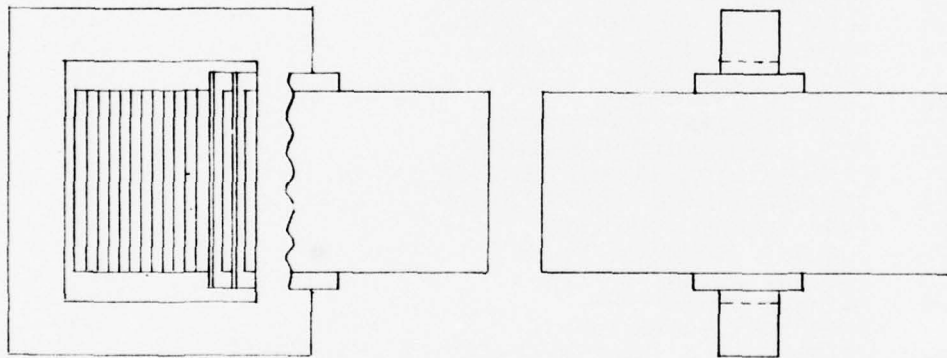
10 KVA   10 KHz
INVERTER TRANSFORMER
CORE/COIL ASSY.

ORTHONOL CORE

Fig. 3-4
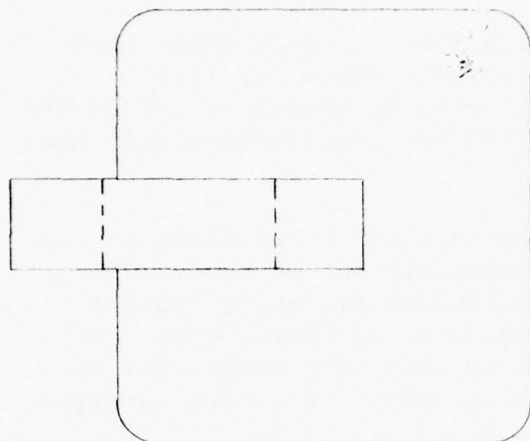
SCALE : FULL
SP. WT. = 0.25 LB/KVA
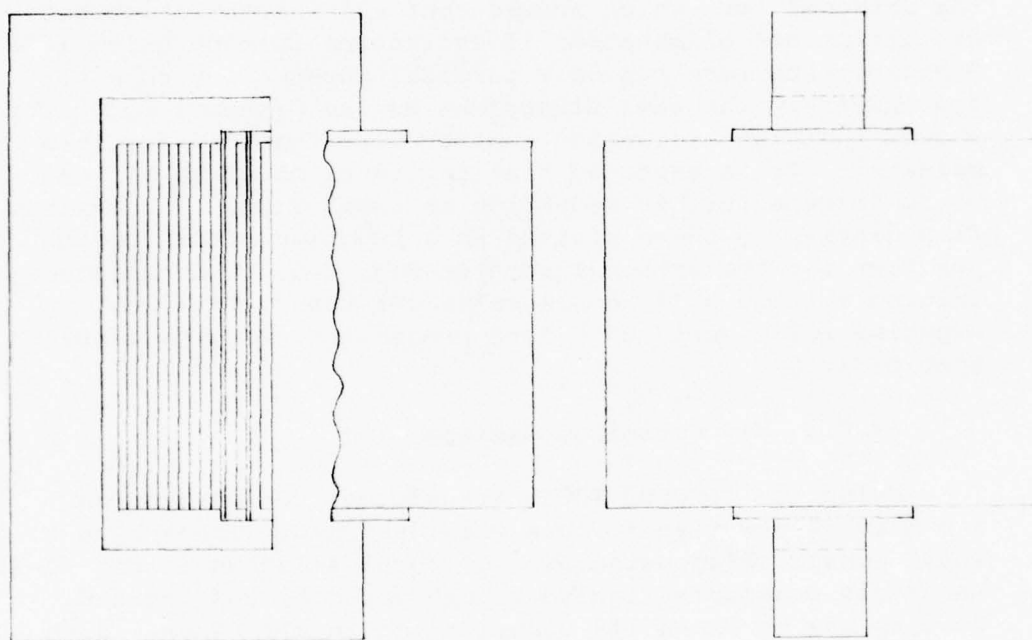
10KVA   10KHz
INVERTER TRANSFORMER
CORE/COIL ASSY.
FERRITE CORE

Fig. 3-5

It appears from this data that orthonol cores show significant advantages over ferrite cores for this application. Additional data will be generated for 10 KVA, 5 KHz transformers, and for 200 KVA transformers with heat exchangers.

All major parts and materials for fabrication of the 10 KW transformer/rectifier assembly are on hand. The primary coils will be wound with #20 AWG heavy Formvar wire. A special double coated wire by Viking Corp. which has the property of self bonding has been chosen for the secondary windings. The mandrel parts have been submitted to U.B. for fabrication.

Detailed specification of the individual windings had been with held pending the outcome of the review meeting at AFAPL. Following the meeting, additional tests were made of the Orthonol core which showed that all instabilities and distortion are eliminated, if excitation is kept below 14KG. Similar tests were run on a toroidal Supermalloy core of approximately the same dimensions as the Orthonol core, which showed that the excitation must be less than 8KG for this material. It is expected that introduction of an air gap would force a further reduction in excitation. The maximum flux density is shown plotted as a function of RMS volts per turn for the Orthonol core in Fig. 3-6. The expected induced voltage will be 3.2 volts per turn. This was experimentally verified before proceeding with the winding specification.

3.2.2 New Optimized Designs

Using the CDC6600 TDOP2 transformer design program, a number of new transformers were designed. These have a shell construction using two "C" cores as shown in Fig. 3-7. Materials considered included both Orthonol and ferrite. Cooling was by Freon 113 vaporization in all cases. Both special and standard cores were considered. It was found that several standard cores could be used without a substantial sacrifice in overall weight. Some of the more interesting designs are listed in Table 2. These are all for layer wound coils. A program modification to permit consideration of pie wound coils in this program would be desirable prior to designing the 200 KW unit.
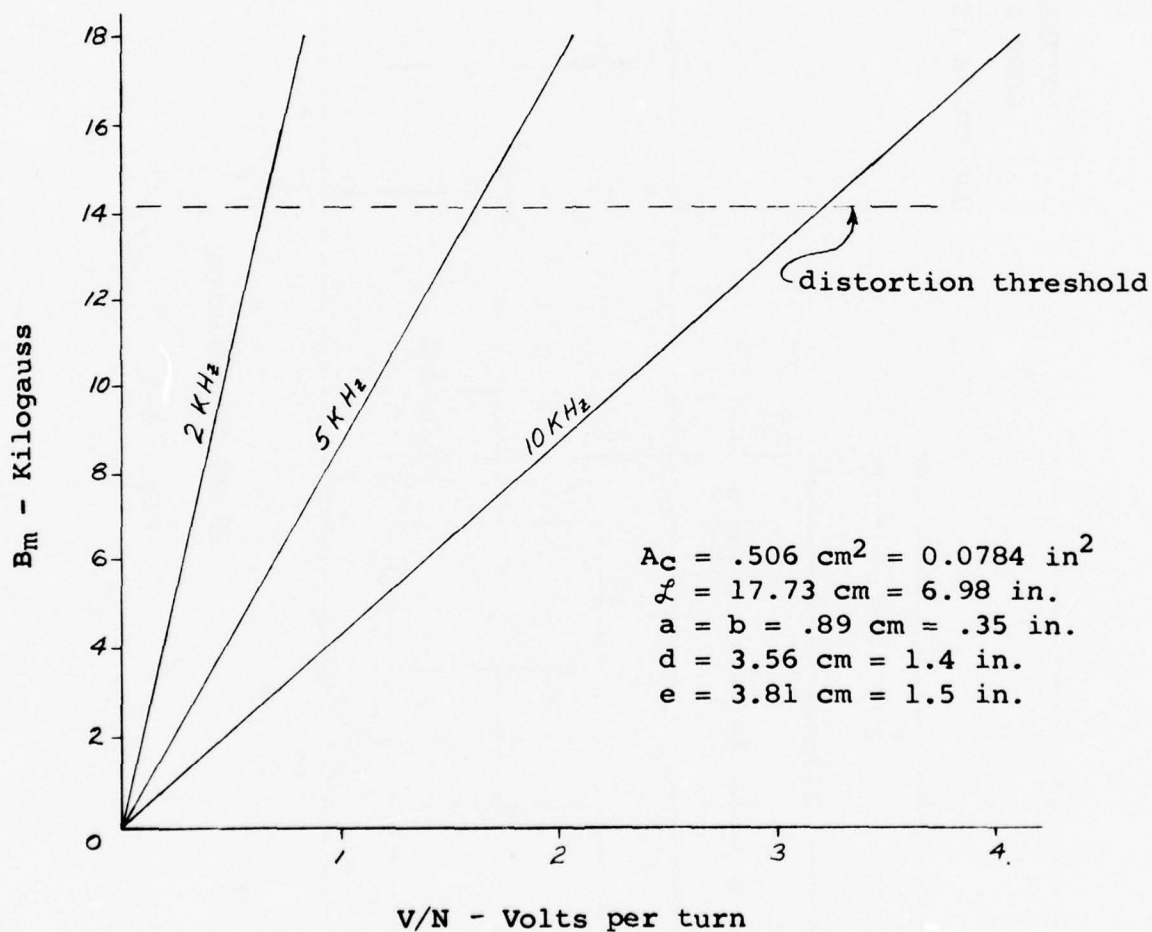
Maximum Flux Density-vs-Volts Per Turn For Orthonol Core

Fig.   3-6

OPTIMAL DESIGN - 1

CORE ASSEMBLY

See Table II For Dimensions
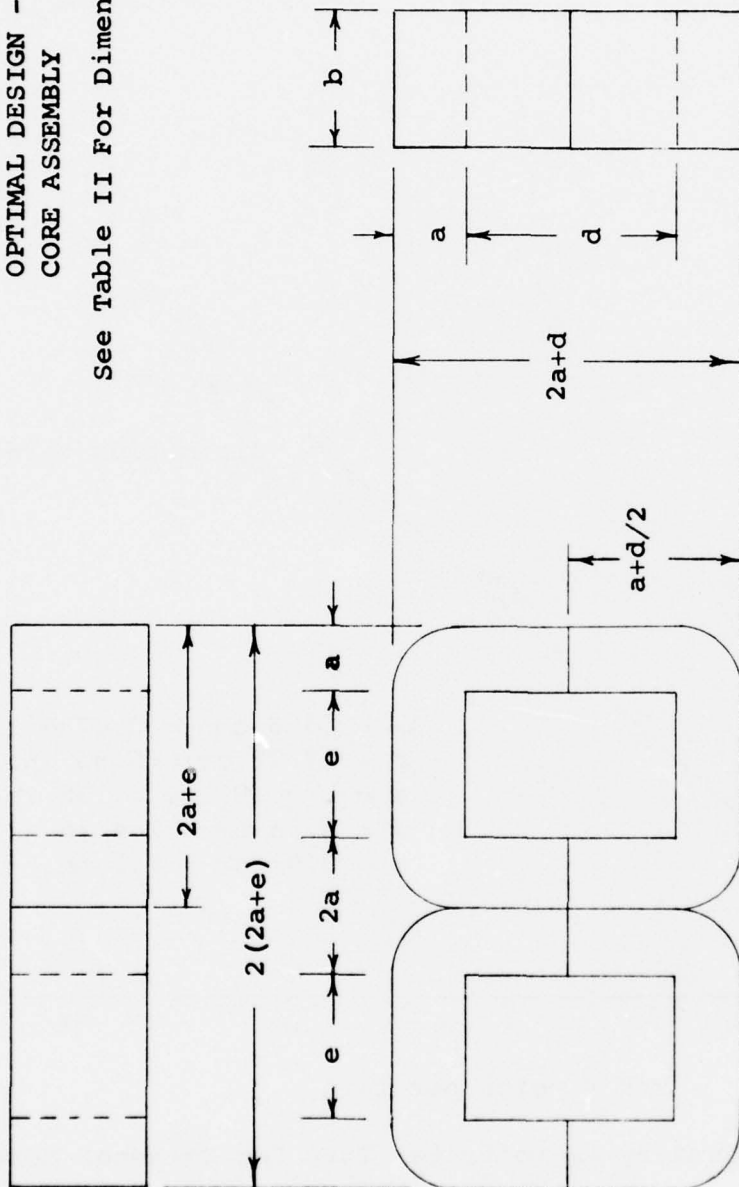
10 KW Core Design

Fig. 3-7

TABLE II
Design Data

Material	Part No.	a	b	d	e	WT.Lb.	eff.%
Orthonol	Special	.775	.775	1.205	.802	1.43	94
Ferrite	Special	1.323	1.323	1.892	1.333	5.08	92
Ferrite	Special	1.414	1.414	2.912	0.957	5.86	94
Orthonol	Special	0.75	0.75	0.988	0.836	1.06	96
Orthonol	MC-1391	1.00	0.75	1.300	0.870	1.779	95
Orthonol	Special	.5916	.5916	1.232	0.905	0.95	95

3.2.3 Fabrication and Testing

As the fabrication of the 10KW transformer proceeded and the personnel became more proficient in the assembly of the unique structures involved, several new fabrication techniques were conceived. The first coil, (Fig 3-8) was constructed in a manner similar to the 50 KVA, 400 HZ transformer. It had windings layered back to back with paper insulation between. Each pair of layers was then separated from the next pair by 1/16" square wood spacers. The final assembly was then vacuum impregnated with varnish. It was found that although this coil occupied only slightly more than half of the core window, it had wide variations in cooling passage dimensions and thus would tend to allow non uniform cooling. The second coil wound (Fig. 3-9) was made with individual single layers separated by 1/16' square wood spacers. A transformer with this coil was installed in a case for testing in Freon 113.

During the period when these coils were being fabricated, the techniques for fabrication of pie wound coils were being developed. Difficulties with mandrel alignment, tensioning, precuring, and handling have all been solved. A complete set of secondary windings have been fabricated as shown in (Fig. 3-10). These are made of #34 AWG double coated wire which can be made to self bond in a precuring operation. Unfortunately, double coated wire is not available in sizes above #23 AWG and even this is only available in 1,000 lb. lots. Therefore, a new spoked mandrel is being fabricated which will permit temporary bonding of pie wound coils with any size wire.

First Layer Wound Coil
Fig. 3-8
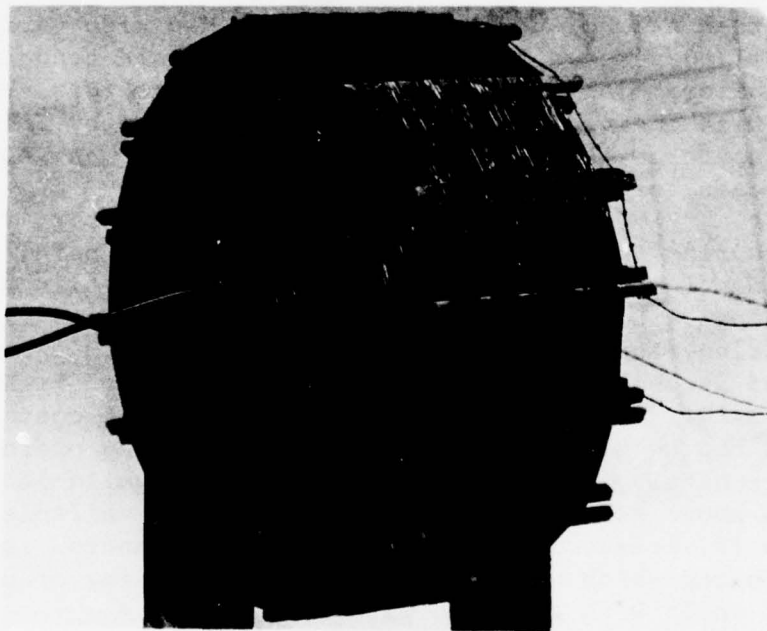
Second Layer Wound Coil
Fig. 3-9
40
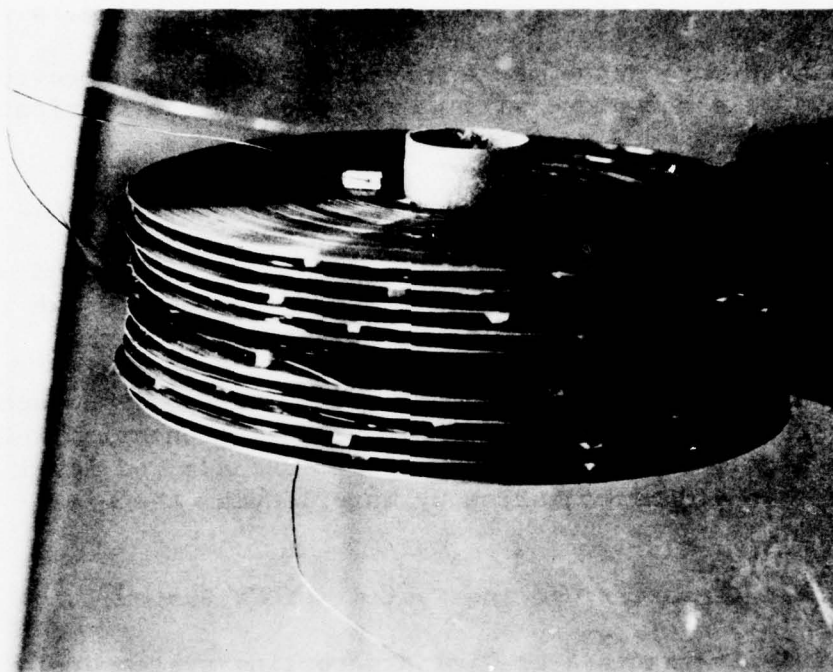
Pie Wound Secondary Coils

Fig. 3-10

In the course of experimenting with pie winding, a technique for multiple layering was developed which permits much more dense packing of the wire than previous methods. This technique will be employed in the fabrication of all pie wound coils in the future.

The second layer wound transformer was installed in a temporary container and successfully tested at full rated current with 60 HZ excitation on both primary and secondary windings to cancel the flux in the core. The total loss was 770 watts which is slightly above the predicted loss of 682 watts. This will be drastically reduced with the new pie windings. The leakage inductance of this transformer was found to be 25.3 microhenries which is also high. This will be reduced to the desired level of less than 4.0 microhenries by interleaving the pie windings.

3.2.4 Inverter Cooling System - 10KW System

The following is a preliminary cooling system design for the 10 KW inverter transformer/rectifier, and analysis of that design.

Input Data and Assumptions

Transformer

Copper Loss	511 Watts
Core Loss	59
Total Dissipation	570

Internal Height	2.30 Inches
Internal Depth	2.49
Internal Width	3.75 (4.00 with clearance)

Rectifiers

Type: (4) Unitrode 687-8 series
Approx total dissipation = 1.1 x 13 x 1 x 8 = 114.4

Overall Height	2 x 1.14 =	2.28
Overall Depth	2 x .75 =	1.50
Overall Width		3.015

Note that the height and width package dimensions are determined by the transformer.

Total Power = 570+114.4 = 684.4, say 700 watts

42

Package internal depth:

Transformer	2.49	Inches
Rectifiers	1.50	
Clearances	.38	
Total	4.38	

Cooling System: Use heat sink finned on both sides, machined as required to form the top surface of the T/R unit. Cooling air will be provided by a blower arranged for impingement flow (cooling air flow from blower is normal to the finned heat sink base area.).

For initial design analysis, use Thermalloy extrusion #6462 heat sink (.250 spaces, .125 thick fins, .655 in deep fins).

Condensing Side

Internal plan area of T/R unit = 4.18 x 4.00 inches
Condenser area = no. fins x area/fin + base area
No. fins in 4 inch width = 10
Area/fin = 4.38 x 0.655 x 2 = 5.74 sq.in
Total area = 10 x 5.74 + 4 x 4.38 = 74.90 sq in $\approx$ 0.5 sq.ft.

Condensing heat transfer coefficient, h_c

$$h_c = 0.943 \left[\frac{p_L (p_L - p_V) g\, h\, k^3}{\mu_L L \Delta t} \right]^{0.25} \qquad (22)$$

where   F113
p_L = liquid density, lb/cu.ft.   97.69
p_V = vapor density, lb/cu.ft   0.461
g = gravity constant, ft/hr^2 4.173 E8
h = heat of vaporization, BTU/lb.   63.12
k = thermal conductivity, BTUh/(F-ft)   0.038
μ_L = viscosity, lb/(ft-hr)   1.646

then
$$h_c = 284.98 \left(\frac{1}{L \Delta t} \right)^{0.25} \qquad BTUh/(sq\,ft \cdot F) \quad (23)$$

43

For L = 0.655 inches = 0.546 ft.

$$h_c = 337.08/\Delta t^{0.25}$$

Since $Q = hA \Delta t$,   (24)

$$(t_F - t_C) = Q/hA$$ (25)

Where

   t_F = fluid temperature, F
   t_C = condenser or case temperature, F
   Q = thermal load, BTUh
   A = condenser area, sq. ft.

$$t_F - t_c = (700)\left(\frac{2}{17}\right)(3.413)(t_F - t_c)^{0.25}/337.08$$ (26)

$$(t_F - t_c)^{0.75} = 0.953$$ (27(

$$t_F - t_c = 0.94 \; F$$ (28)

External Forced Air Cooling

   Assume Rotron "Spartan" fan, type S, motor series 682YS
   Operating point = 50 CFM @ .175 inches water
   Forced air heat transfer coefficient:
      No fins on air side (4.687 wide) = 12
      Effective area = $12 \times .655 \times 2 \times 4.687 + 4.687^2 \times 2/3 = 88.3$ sq.in.
      Total flow area (two directions)= $0.25 \times 0.655 \times 12 \times 2 = 3.93$ sq in.
      At 50 CFM, air velocity = $V = (50) \times 144/3.93 = 1832$ ft/min
      At assumed average air temp of 110F,
         air density = 0.0696 lb/cu ft
         air viscosity = 0.0465 lb/(ft-hr)
      Equivalent diameter = $4 \times 0.25 \times 0.655/(2 \times (0.25 + 0.655)) = 362$ in =
                                                                               .03 ft. (29)
      Re = Reynolds no. = $.0696 \times 1832 \times 60 \times .03/.0465 = 4936$ (30)
      $h = 0.023 \, k/D \, Re^{0.8} Pr^{0.4}$ (31)
         = $0.023 \times 0.0160/0.03 \times 4936^{0.8} \times 0.7^{0.4} = 9.61$ BTUh/(sq ft-F)   (32)

44

Since $Q = hA\left(t_c - t_a\right)$, $\qquad$ (33)

$$t_c - t_a = Q/(hA) \qquad (34)$$

where

t_c = case temperature, F
t_a = air temperature, F
h = heat transfer coefficient, BTUh/(sq ft-F)
A = heat transfer area, sq ft.

$$t_c - t_a = (700)\left(\tfrac{2}{17}\right)\left(3.413\right)\Big/\left[(9.61)(88.3/144\right] = 47.7\,F \quad (35)$$

The fluid temperature will average 47.7 + 0.9 = 48.6F above the ambient air temperature, after repeatable cyclic conditions have been attained. Assuming a maximum ambient temperature of 100F, the fluid temperature of approximately 150F will generate an internal pressure of approximately 15 PSlG.

A more detailed transient thermal analysis will be performed later in the program to determine the rate of cyclic temperature increase and the peak temperature excursion over the average.

The attached Figure 3-11 indicates the general outline of the T/R system. The figure is a preliminary concept, not necessarily to scale, and not necessarily reflecting the final design. For example, the condensing fins appear much longer than necessary, considering the low temperature drop across the condensing surfaces. It is likely that these fins will be reduced in length in the final design, reducing the overall height somewhat.

3.3 Dynamic Analysis Programs

3.3.1 Characteristics of Magnetic Cores

The directly measureable characteristics of transformers, while exhibiting certain nonlinearities, must be altered either by signal processing or computation to yield information

AIR IN

AIR OUT

XFRMR
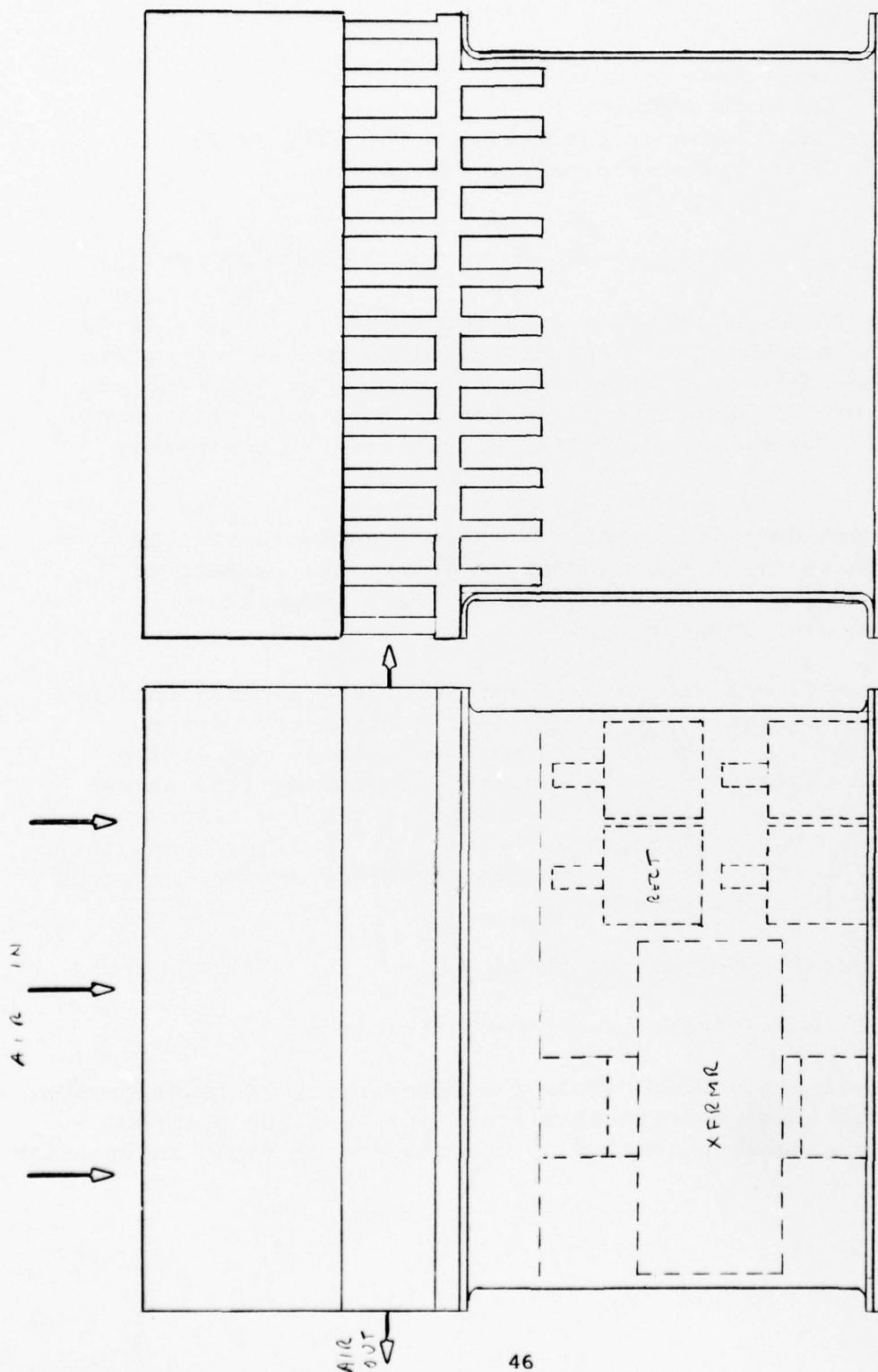
RECT

Preliminary Layout 10 KW Inverter

Transformer, Rectifier, and Freon to Air Cooled Condenser

Fit. 3-11

46

on the properties of the feromagnetic materials. Each manufacturer has a preferred set of tests for core evaluation depending on the particular application. IEEE standards 164 and 106 describe in some detail the particular tests which are deemed acceptable, but the degree to which they are applied seems to vary from one manufacturer to another. A list of tests which have been implemented at TTL is shown in Table 3. Additional tests for pulse and biased core transformers are described in references[1]through[4].

TABLE 3

Magnetic Device Tests

1. Core Loss and Volt-Ampere Test (open circuit test)
2. Winding Loss Test (Short circuit test)
3. Sine Voltage Tests (B-H curve and V-I curve)
4. Sine Current Tests (B-H curve and V-I curve)

The specific materials tested at TTL have been limited to tape wound cores having lamination thicknesses from $\frac{1}{2}$ to 4 mils. The materials used in these tests were Orthonol (50% Nickel, 50% Iron), Magnesil (3% Silicon, 97% Iron), and Supermendur (49% Cobalt, 49% Iron, 2% Vanadium). A few samples of Permalloy (79% Nickel, 17% Iron, 4% Molybdenum) and Supermalloy (78% Nickel, 17% Iron, 5% Molybednum) were tested along with two ferrite cores, but the most extensive testing was performed on the first three materials mentioned.

The purpose of these measurements was to obtain data for development of a mathematical model for transformers which included the nonlinear properties of their cores. This, of course, was not the first attempt that had ever been made to model magnetic materials properties. It was shown by Manly (Ref 6) that models based on the hyperbolic tangent, arctangent, and lognormal functions fall short of accurately representing the core properties. He pointed out that even models which appear to closely fit measured hysteresis curves fail to match the I-V characteristics. Other models which have been developed include exponential series (Ref 7); rational fractions (Ref 8), and least

47

square curve fitting routines (Ref 9). Since none of
these were easily adapted to the requirements of a
transformer analysis and design program using minimal
computing equipment, an effort was undertaken to develop
a satisfactory model.

Such a model has been developed by TTL and its utility
in transformer analysis has been demonstrated. The transition
from dynamic analysis to design has not been made. So at
this writing, it has not been established that a transformer
can be synthesized from the TTL model.

The TTL Model

The TTL model is generated from three experimentally
determined parameters.   These are the coercive force, the
saturation flux density, and residual flux density. The
mathematical form on which it is based is $y = x/(a + x)$ (36)
where x is a function of the magnetic field intensity.
This function has the value zero at $x = 0$ and approaches
± 1 as x becomes large in either the positive or negative
directions. Its resemblence to a magnetization curve was
one reason it was chosen as the basis for the model. The
mathematical expressions for various core properties are
shown below.

BH Curves

The major loop is modeled as shown in Equation (37)

$$B = B_s \left(H + K H_c \right) \Big/ \left[H_c \left(\frac{B_s}{B_R} - 1 \right) + \left| H + K H_c \right| \right]$$ (37)

This Equation exactly matches experimental data at the
points $(H_c, 0)$, $(0, B_r)$, (∞, B_s). The symbol k, has a value
of -1 for the lower or right hand curve and +1 for the
upper or left hand curve. To represent a minor loop, the
upper and lower curves are shifted toward each other by
equal amounts such that they intersect at the points
$(\pm H_m, \pm B_m)$. This shift is represented by a term

48

designated the displacement flux density, B_0.

Equations (38) and (39) can be used to generate a complete set of B-H curves as shown in Fig. 3-12.

$$B = B_S \left(H + K H_c \right) \Big/ \left[H_c \left(\frac{B_S}{B_r} - 1 \right) + \left| H + K H_c \right| \right] - K B_0 \tag{38}$$

$$B_0 = \frac{1}{2} \left[\frac{B_S \left(H_m + H_c \right)}{H_c \left(\frac{B_S}{B_r} - 1 \right) + \left| H_m + H_c \right|} - \frac{B_S \left(H_m - H_c \right)}{H_c \left(\frac{B_S}{B_r} - 1 \right) + \left| H_m - H_c \right|} \right] \tag{39}$$

Magnetization Curve

The magnetization curve Equation (40) is modeled as the locus of the points (H_m, B_m) from Equations (38) and (39).

$$B_m = \frac{1}{2} \left[\frac{B_S \left(H_m + H_c \right)}{H_c \left(\frac{B_S}{B_r} - 1 \right) + \left| H_m + H_c \right|} + \frac{B_S \left(H_m - H_c \right)}{H_c \left(\frac{B_S}{B_r} - 1 \right) + \left| H_m - H_c \right|} \right] \tag{40}$$

H-VS-B

The inverted form of Equation (38) is shown in Equation (41)

$$H = H_c \left(\frac{B_S}{B_r} - 1 \right) \left(B + K B_0 \right) \Big/ \left[B_S - \left| B + K B_0 \right| \right] - K H_c \tag{41}$$

This form is particularly useful for determination of the current from a known flux waveform.

Core Loss

Since the model represents a continuous closed hysteresis loop, the integral over one complete cycle will yield an expression for the core energy loss per unit volume.

$$e_h = 2 B_S \left[\left| H_m + H_c \right| - \left| H_m - H_c \right| + C \ln \left(\frac{C + \left| H_m - H_c \right|}{C + \left| H_m + H_c \right|} \right) \right] - 4 B_0 H_m \tag{42}$$

49

0.5 Oe/Div.

$B_s = 18$ kG

$B_r = 15.3$ kG

$H_c = 0.65$ Oe.

5 kG/Div.
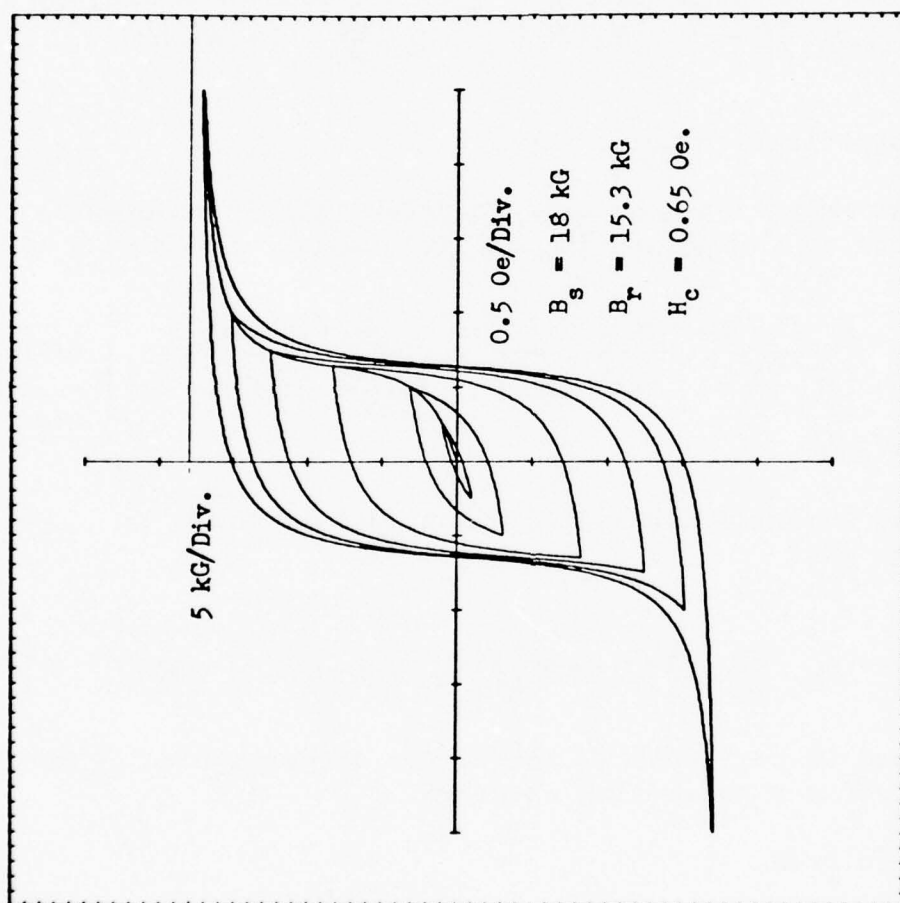
Computed Hysteresis Curves for Magnesil

Figure 3-12

50

If the parameters used for B_s, B_r, and H_c are for some frequency, F, then the total core loss will be represented by the product of Equation (42) and the frequency. For dc data, Equation (42) represents only the hysteresis loss and the loss at frequencies other than zero must include a term for eddy current loss such as shown in Equation (43).

$$ P_e = \frac{1}{6\rho} \left(\pi f \tau B_m \right)^2 \tag{43} $$

Permeability

The incremental permeability may be modeled by differentiation of Equation (38). The result is shown in Equation (44).

$$ \frac{dB}{dH} = \mu \left[B_s H_c \left(\frac{B_s}{B_r} - 1 \right) \right] \bigg/ \left[H_c \left(\frac{B_s}{B_r} - 1 \right) + |H + K H_c| \right]^2 \tag{44} $$

Since the incremental permeability approaches zero as the magnetic field intensity approaches infinity, the permeability of free space, μ_o, is added to Equation (44) to model the total permeability of the material.

A term often used to describe rectangular core materials is the squareness ratio, B_r/B_s. This quantity approaches unity for a perfectly rectangular core. The ratio of the permeability at H = 0 to that at H = H_c is

$$ \mu_r \big/ \mu_c = \left(1 - \frac{B_r}{B_s} \right)^2 \tag{45} $$

From this Equation it can be seen that for a squareness ratio of 0.9 the slope of the sides of the modeled loop is one hundred times that of the ends. Thus the model is capable of representing extremely square materials, a property which is lacking in most other core models.

51

I-V Characteristics

Two limiting cases occur for a driven core. They are voltage source and current source conditions, both of which are ideal cases. In Ref. 6, a sinusoidal current source given by

$$I = I_m \sin \omega t \qquad (46)$$

which would force K to have the form

$$K = \cos \omega t \Big/ |\cos \omega t| \qquad (47)$$

It may be shown that the induced voltage for a core of cross-section, A_c, and magnetic path length, $\mathcal{L}$, is given by

$$V_L = - \frac{N^2 A_c}{\mathcal{L}} \mu \omega K \left(I_m^2 - I^2 \right)^{\frac{1}{2}} \qquad (48)$$

The derivation of VI characteristics for a voltage source requires the numerical integration of a first order differential Equation, and is discussed in the section on dynamic modeling.

Comparison of Model with Experimental Data

Experimental and computed hysteresis curves are shown in Fig. 3-13 for Supermendur at 77°K. It appears that the slope of the sides of the computed curve are less than that of the data. This problem is due mainly to the fact that the value of B_S is hard to determine since it is not possible to drive H to infinity. An alternative would be to measure the permeability at $H = H_c$, and to compute the saturation flux density from

$$B_S = \mu_{H_c} H_c B_r \Big/ \left(\mu_{H_c} H_c - B_r \right) \qquad (49)$$

52

This yields a value of $B_s = 1.59T$, whereas the value used in computing Fig. 3-13 was 1.7T. The recomputed hysteresis curve is shown in Fig. 3-14.

Data for a Magnesil core with the following Table 4 specifications, are shown in Fig. 3-15.

TABLE   4

Magnesil Core Type 50086-2K

$$N = 50$$
$$A_c = 4.3 \times 10^{-6}$$
$$\mathscr{L} = 8.47 \times 10^{-2}$$
$$B_r = 1.5T$$
$$H_c = 43.9 \text{ at/m}$$
$$B_s = 1.79T$$
$$f = 60 \text{ HZ}$$

The top curve is hysteresis and the lower curve is the I-V characteristic, both were taken at five different values of magnetic field intensity. The computed BH curves and I-V characteristics are shown in Fig. 3-16. The most obvious discrepancy is in the curvature of the peaks of the I-V characteristics. This is thought to be due to the fact that the source was loading slightly at the peak so that the current was slightly non-sinusoidal. This theory is supported by the analysis for the constant voltage case which shown considerable rounding of these curves.

Examination of the computed I-V characteristic shows a discrepancy with experimental data in that the peak values are shifted to the left much more in the data than in the computed curves. Examination of the B-H curves shown the same phenomenon. Namely the H axis intercepts, H_c, are all much closer to the H_c in the computed results than in the data. Experimental and computed values of H_c - vs - H_m are shown in Fig. 3-19. From this curve it is seen that the TTL model in its present form deviates considerably from the experimental data. Residual magnetization, B_r, is
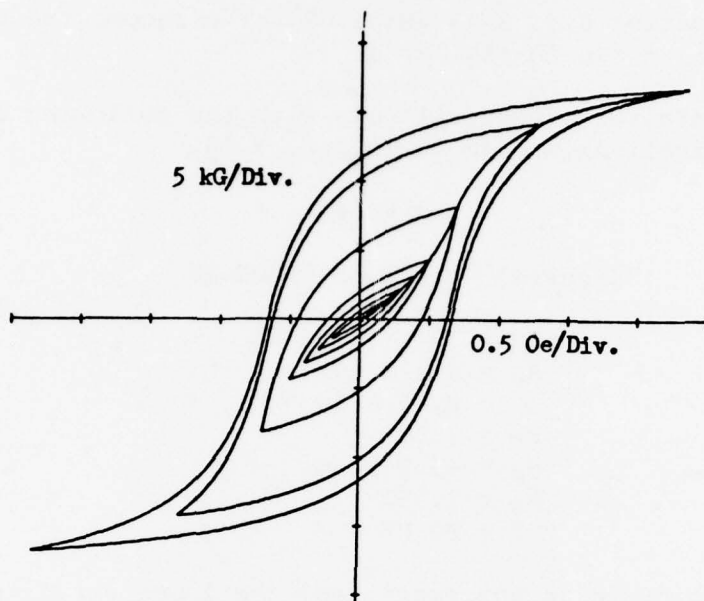
Computed Hysteresis Curves for Supermendur at 77° K
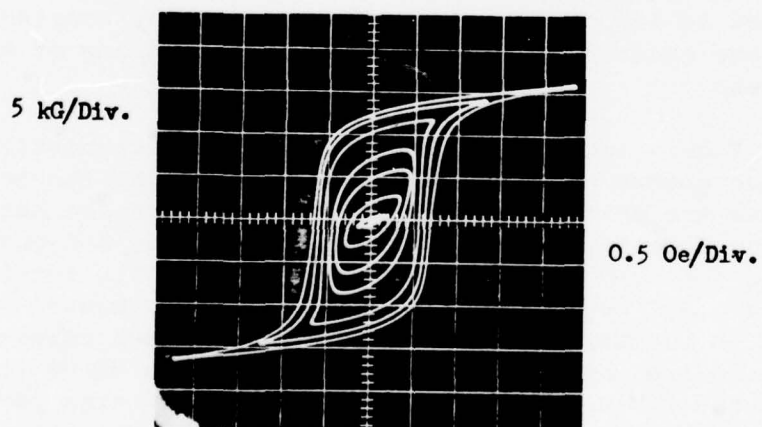
Measured Hysteresis Curves for Supermendur at 77° K

Figure 3-13

54

$$\frac{B_r}{B_s} = 0.78566$$

5kG/Div.

0.5Oe./Div
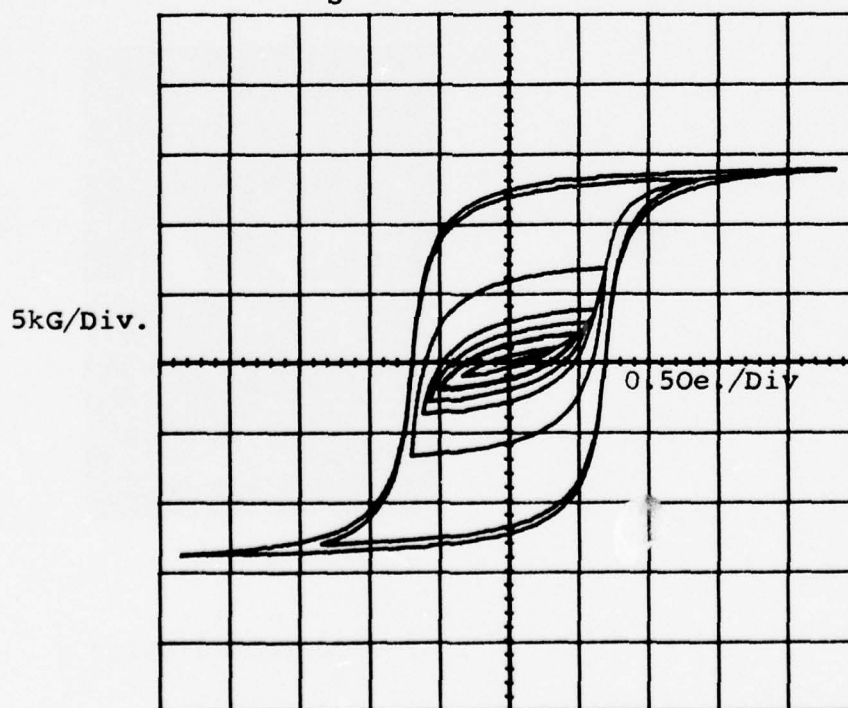
Recomputed Hysteresis Curves for Supermendur at 77K.

Figure 3-14

B,
0.67 T/Div

Core Properties
50086-2k
N = 50 turns
A_C = 4.3X10^{-6}m^2
$\mathcal{L}$ = 8.47X10^{-2}m
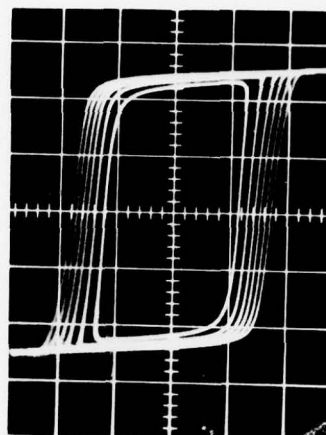
H, 29.5 At/Div. or
I, 0.05 At/Div.

B-H Curves
(a)

V,
0.5 V/Div.
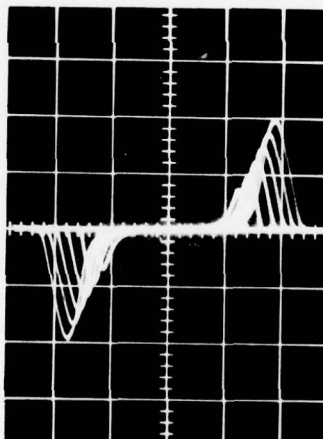
I, 0.05 A/Div.

I-V Characteristics

Electrical and Magnetic Properties of Magnesil

Figure 3-15

56
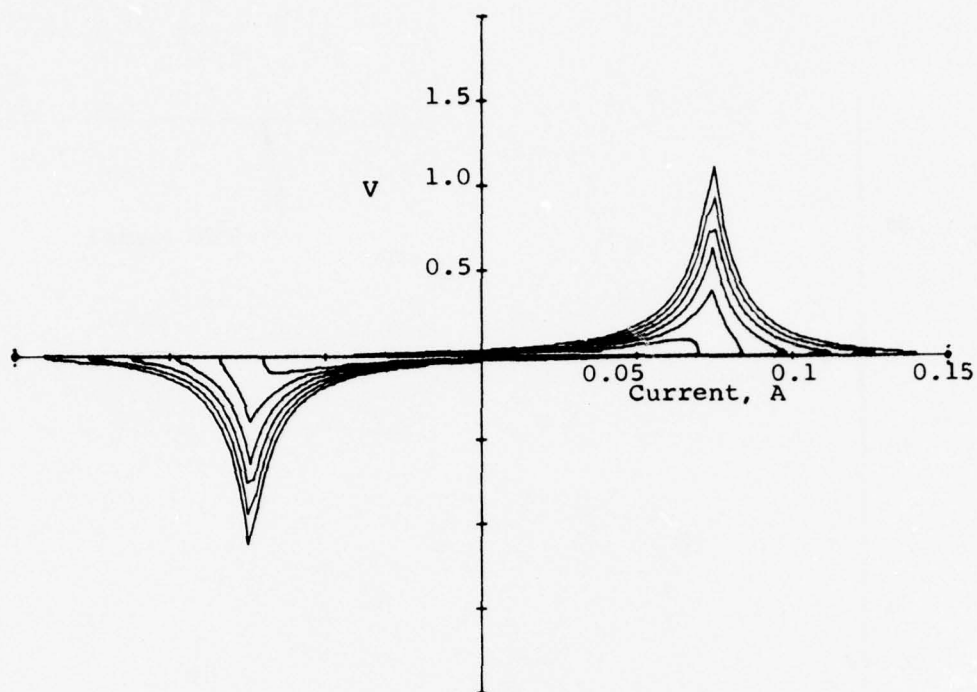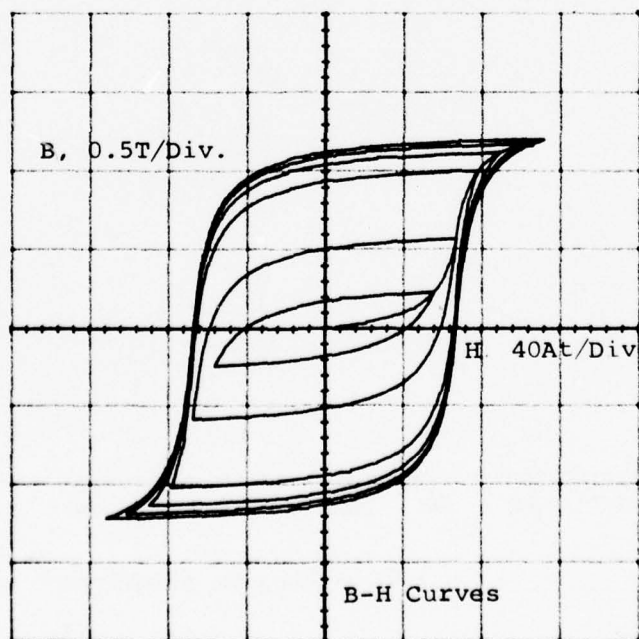
I-V Characteristics

Computed Electrical Characteristics of Magnesil
Figure 3-16
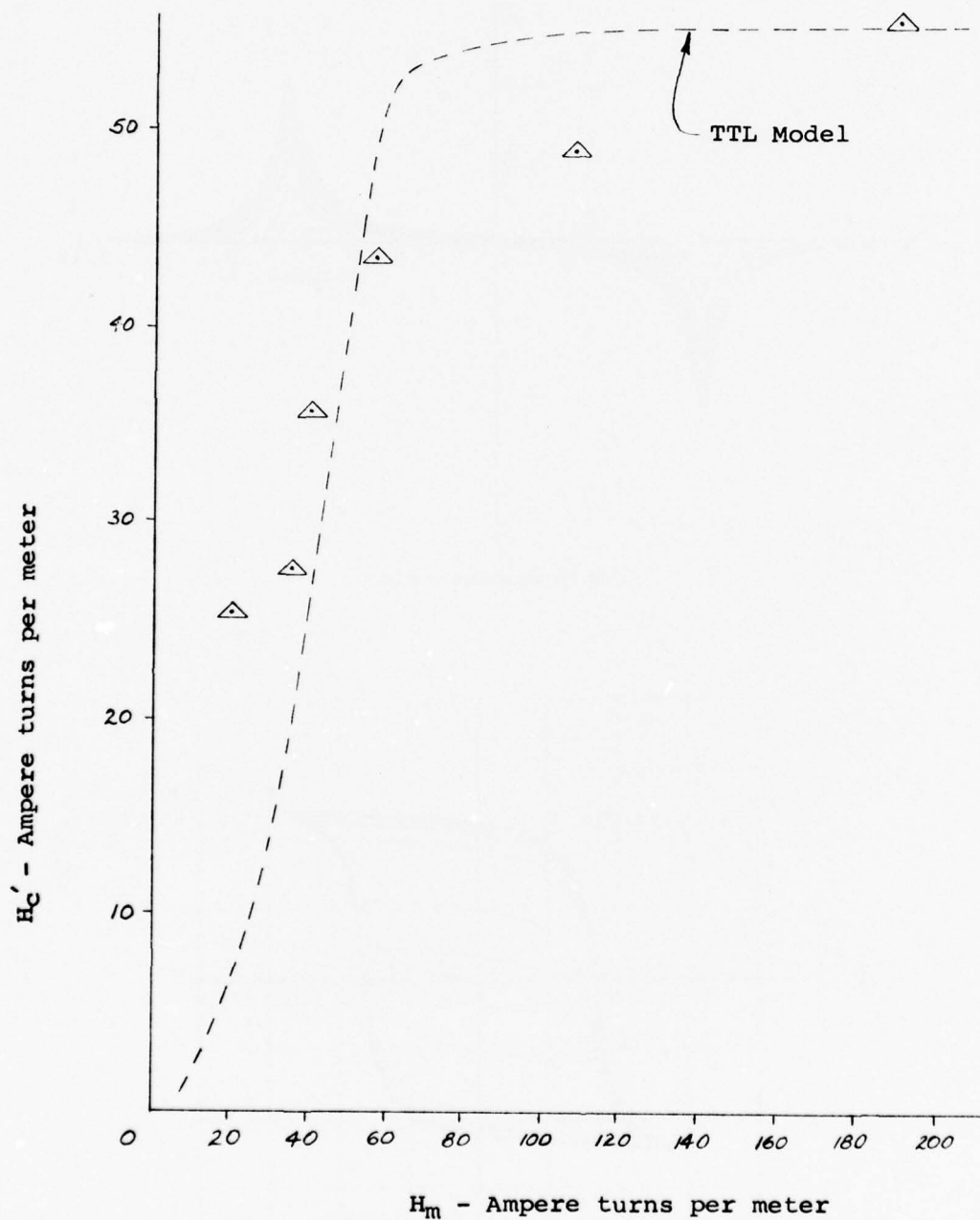
Experimental and Computed H_C' - vs - H_m for Magnesil

Fig. 3-17

58

plotted as a function of maximum flux density, B_m, in Fig. 3-18. Here it is seen that agreement between theory and experiment is excellent. A number of modifications have been attempted to correct the model by altering the H_c term in the Equation as a function of H_m. The results of two of the more promising approaches are shown in Fig. 3-19. It is seen that the correction

$$H_o = \left[H_c * H_m \right] \Big/ \left[H_m + H_c \left(\frac{B_s}{B_r} - 1 \right) \right] \tag{50}$$

has little or no effect on the curves while the correction

$$H_o = \left[H_c * H_m \right] \Big/ \left[H_m + H_c \right] \tag{51}$$

tends to reduce the H axis intercept too much. There is some question as to the importance of this problem since the electrical behavior is determined primarily by the maximum flux density and the instantaneous permeability. These two characteristics are accurately represented by the present model. While high accuracy is desirable in modeling all aspects of the material characteristics it may not be required in the present program.

3.3.2 The Dynamic Model

The basic nonlinear transformer model is shown in Fig. 3-20.
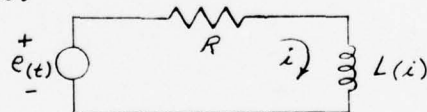
Fig. 3-20

Basic Model - Core Only

The describing differential Equation is

$$L(i) \frac{di}{dt} = e(t) - Ri \tag{52}$$

where $e(t)$ is (usually) a sine wave input. Given that

59
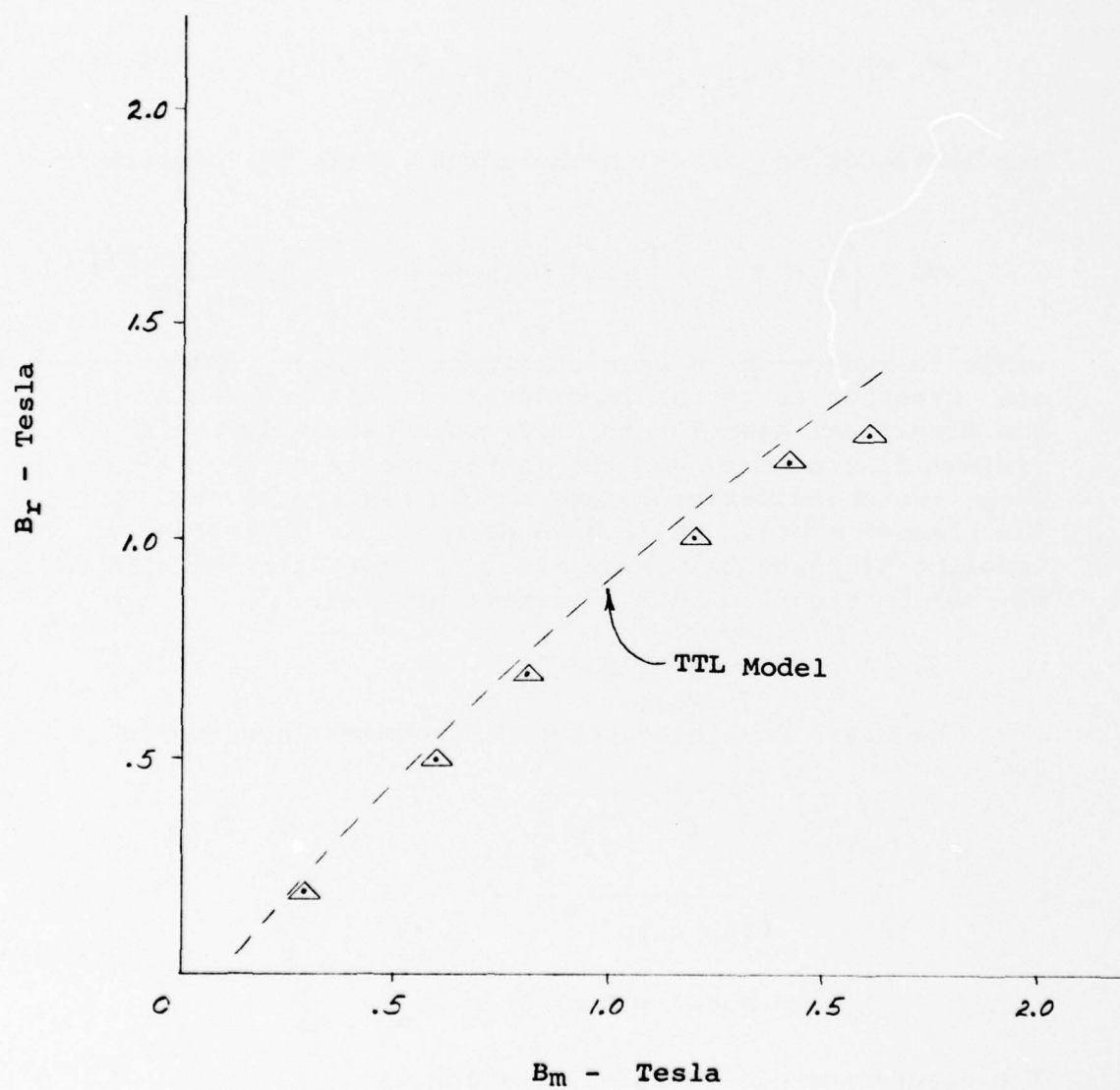
Experimental and Computed B_r-vs-B_m Data for Magnesil

Fig. 3-18

Figure 3-19

Modified BH Curves Compared to Original   Model

Within the figure:

ORIGINAL

$$H_0 = \frac{H_C * H_M}{H_M + H_C}$$

$$\frac{H_C * H_M}{H_M + H_C \left(\frac{BS}{BR} - 1\right)}$$
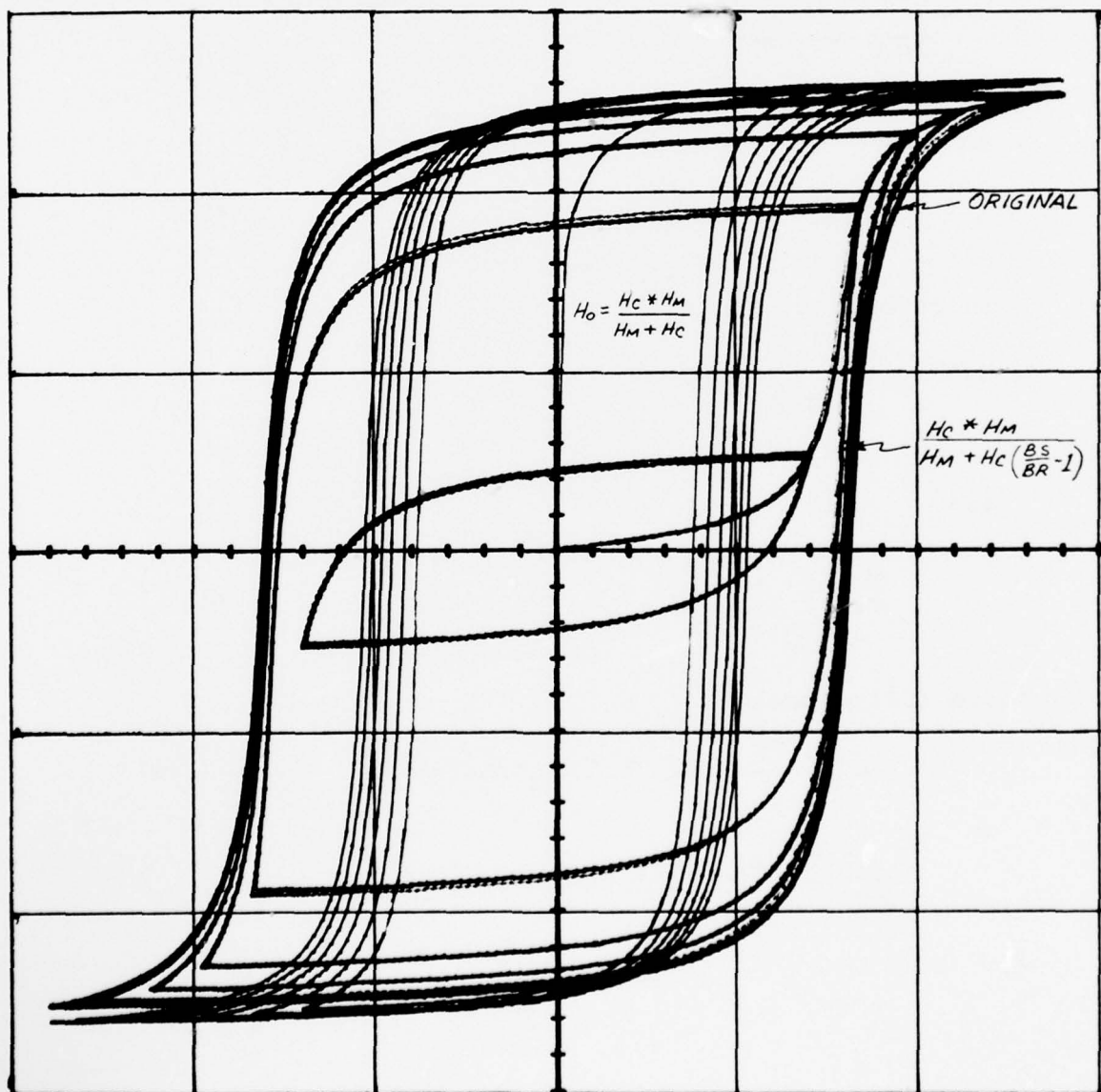
$$e_{(t)} = V_0 \sin \omega t \tag{53}$$

where

$$\omega = \frac{2\pi}{T} = 2\pi f_0 \quad RAD/SEC. \tag{54}$$

we will find it convenient to effect a change of time
scale so that one period of the sine wave requires one
second in terms of a new time variable τ . Let

$$2\pi t = 2\pi \tau \tag{55}$$

so that

$$2\pi f_0 t = 2\pi \tau \tag{56}$$

therefore

$$\tau = f_0 t \tag{57}$$

and

$$\frac{d\tau}{dt} = f_0 \tag{58}$$

Equation (52) becomes

$$L_{(i)} \frac{di}{dt} \cdot \frac{d\tau}{dt} = e_{(\tau)} - Ri \tag{59}$$

or

$$\frac{di}{dt} = \frac{e_{(\tau)} - Ri}{f_0 L_{(i)}} \tag{60}$$

62

Equation (60) is the basic Equation which was programed for the HP 9830 (the HP 9830 uses a modified basic language).

The nonlinear model of the core, $L(i)$, is defined by the equation

$$L(i) = \frac{N^2 A_c \mu_o}{\mathcal{L}} + \frac{\frac{N^2 A_c \mu_o}{\mathcal{L}} H_c \left(\frac{B_s}{B_r} - 1 \right)}{\left[H_c \left(\frac{B_s}{B_r} - 1 \right) + \left| \frac{Ni}{\mathcal{L}} + K H_c \right| \right]^2} \qquad (61)$$

where, for illustrative purposes, values in Table 5 have been used as the parameters of the model:

$$
\begin{aligned}
N &= 50 \\
A_c &= 4.3 \times 10^{-6} m^2 \\
\mathcal{L} &= 8.47 \times 10^{-2} m \\
\mu_o &= 4\pi \times 10^{-7} H/m \\
B_s &= 1.8 T \\
B_R &= 1.5 T \\
H_c &= 40 \, at/m
\end{aligned}
\quad \left.\right\} \quad
\begin{aligned}
&\text{MAGNETIC CORE} \\
&\text{TYPE 50086-2K}
\end{aligned}
$$

TABLE 5
Model Parameters

Equation (60) can be written as

$$\frac{di}{d\tau} = \frac{i - e(\tau)/R}{-f_o/RL(i)} \qquad (62)$$

and then integrated (graphically) as indicated in Fig. 3-21.

Fig. 3-21

Graphical Integration Procedure

63

Equation (60) gives the slope of a solution curve in the $i(\tau)$ vs τ plane. Given a value of current i at $\tau = \tau_0$ then a line dropped from A to the curve $-\frac{e(\tau)}{R}$ has a length equal to $i - \frac{e(\tau)}{R}$. This defines the point B. Next, on a line parallel to the τ axis lay of a line segment which is equal in magnitude to $\frac{f_0}{R} L(i)$. This defines the point C. By construction, the line A C then has a slope equal to

$$ m = \frac{i - e(\tau)/R}{-\frac{f_0}{R} L(i)} \tag{63} $$

and hence, a "short" tangential segment of the line A C constitutes a solution to Equation (62). One then moves to the endpoint of the short tangential approximation and repeats the procedure to obtain the next approximation to the solution curve. Given that these tangential approximations are "short enough", one obtains an approximation to the true solution curve that can be made arbitrarily close.

The graphical procedure can be implemented as a difference equation on a computer by writing

$$ i_{n+1} = m\left(i_n, n\Delta\tau\right)\Delta\tau + i_n \tag{64} $$

where
$$ m(i_n, n\Delta\tau) = \frac{\frac{V_0}{R} \sin(2\pi\Delta\tau n) - i_n}{\frac{f_0}{R}\left[\frac{N^2 A_c \mu_0}{\mathcal{L}} + \frac{\frac{N^2 A_c \mu_0}{\mathcal{L}} B_s H_c \left(\frac{B_s}{B_r} - 1\right)}{\left[H_c\left(\frac{B_s}{B_r} - 1\right) + \left|\frac{N i_n}{\mathcal{L}} + K H_c\right|\right]^2}\right]} \tag{65} $$

$$ K = -1, \text{ WHEN } \frac{di}{dt} < 0 \tag{65a} $$

and

$$ K = 1, \text{ WHEN } \frac{di}{dt} > 0 \tag{65b} $$

64

When an engineer graphically solves the problem using Equation (62) he learns to adapt the "size" of the tangential approximation to the steepness of the solution curve. That is, for shallow slopes he is willing to let the tangential approximation (the line element CD in Fig. 3-21 be larger than when the slope is "steep". We can approximate the physical feel the engineer develops (who is graphically solving the problem) by using the logic available on a digital computer to permit a variable solution size that is slope dependent. For example, the computer calculates a new point D based on a fixed increment. However, before the point D is used as a new jumping off point in the computation of the solution, the slope of the line CD is checked. If the slope exceeds a specified value, then the $\Delta \tau$ interval is halved and the computation is repeated - starting of course from the same initial point A. This procedure is repeated until the slope falls within the constraint placed on it. Obviously, a compromise must be effected-if we make the slope constraint too severe then the digital process is slowed up and one must pay an excessive price, in terms of computer time, for a degree of precision that may not be warranted.

Given that the current waveform must be recorded at equal time intervals in order to do a time series analysis (for example, a spectral analysis) then the computer must also be programmed to record data only at $\Delta \tau$ second intervals. For this reason, the procedure of halving the intervals is a good one, since the computer can remember the total number of times that the interval was halved and hence record only the $\Delta \tau$ second interval points for later use with, for example, a Fast Fourier Transform routine.

Core Model with Resistive Load Ladder Analysis

The model of Fig. 3-20 can be upgraded to that of Fig. 3-22 in a relatively easy manner. In Fig. 3-22 let the series resistance R become R_1 and call the pure (equivalent) resistive load R_2.
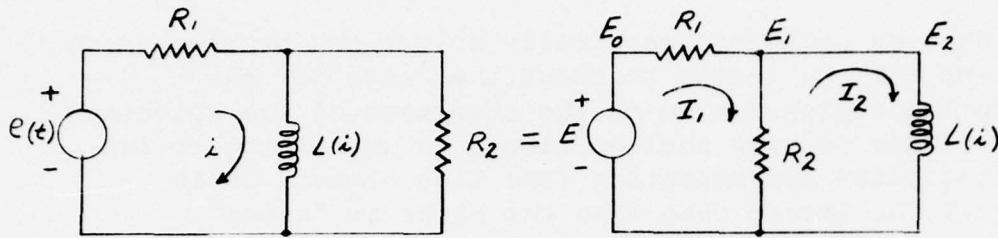
Fig. 3-22

Core with Resistive Load

Using Ladder analysis, we can write

	$\frac{R_1}{R_2} L(I_2)S + R_1 + L(I_2)S$	E_0
R_1	$\frac{L(I_2)}{R_2} S + 1$	I_1
$\frac{1}{R_2}$	$S L(I_2)$	E_1
O	1	I_2
$\frac{1}{L(I_2)}S$	$L(I_2)S$	E_2

TABLE 6

Ladder Analysis of Transformer
with Resistive Load

From Table 6 , it is seen that

$$\frac{I_2}{E_0} = \frac{1}{\left(\frac{R_1}{R_2} + 1\right) S L(I_2) + R_1} \qquad (66)$$

or, in the time domain

$$\left(\frac{R_1}{R_2} + 1\right) L(t_2) \frac{dt_2}{dt} + R_1 i_2 = e(t) \qquad (67)$$

or $\qquad \frac{di_2}{dt} = \dfrac{e(t) \frac{R_2}{R_1 + R_2} - \frac{R_1 R_2}{R_1 + R_2} i_2}{L(i_2)} \qquad (68)$

Accounting for the change of time scale, Equation (68) becomes:

66

$$\frac{di_2}{d\tau} = \frac{e(\tau)\frac{R_2}{R_1+R_2} - \frac{R_1 R_2}{R_1+R_2} i_2}{f_0 L(i_2)} \qquad (69)$$

Therefore the computer program associated with Equation (67) can be used directly by letting

$$e(\tau) \longrightarrow e(\tau) \frac{R_2}{R_1+R_2} \qquad (70)$$

and

$$R \longrightarrow \frac{R_1 R_2}{R_1 + R_2} \qquad (71)$$

Once the magnetizing current is known, the source current and load current can be found from the ladder analysis array of Table 6   From Fig. 3-22 we observe that the source current is I_1 .   From Table 6 we obtain

$$\frac{I_1}{I_2} = \frac{\frac{L(I_2)S}{R_1} + 1}{1} \qquad (72)$$

$$I_1 = \frac{L(I_2) S I_2}{R_2} + I_2 \qquad (73)$$

$$\therefore \quad i_1 = \frac{1}{R_2}\left[e(\tau)\frac{R_2}{R_1+R_2} - \frac{R_1 R_2 i_2}{R_1 + R_2}\right] + i_2 \qquad (74)$$

$$= \frac{e(\tau) + R_2 i_2}{R_i + R_2} \qquad (75)$$

also from Table 6 $\quad I_1 - I_2 = f_0 \frac{L(I_2)}{R_2} \frac{di_2}{d\tau} \qquad (76)$

$$\therefore \ Load\ Current = \frac{e(\tau) - R_1 i_2}{R_1 + R_2} \tag{77}$$

To summarize, the magnetizing current is found by solving

$$\frac{d i_2}{d\tau} = \frac{e(\tau)\frac{R_2}{R_1 + R_2} - \frac{R_1 R_2 i_2}{R_1 + R_2}}{f_0\ L i'(i_2)} \tag{78}$$

for $i_2(t)$. The Load Current is:

$$i_1 - i_2 = i_{Load} = \frac{e(\tau) - R_1 i_2}{R_1 + R_2} \tag{79}$$

and the total current drawn from the source is:

$$i_1 = \frac{e_1(\tau) + R_2 i_2}{R_1 + R_2} = i_2 + i_{load} \tag{80}$$

Note that a "mix" of both frequency domain and time domain notation has been employed to determine the governing differential equation. This "mix" of approaches is an efficient analysis method and produces no error since the final result is written in time domain. In this regard, $L\ (I_2) s$ has been employed as an operator and correct results are obtained given that $L\ (I_2) s$ operates only on I_2 and that the final results are written as differential equations in the time domain.

Core Model With Resistive Load – Equivalent Circuit Analysis

Fig 3-22 can also be analyzed by the use of equivalent circuits. First, convert the voltage source to a Norton equivalent current source (Fig. 3-23).
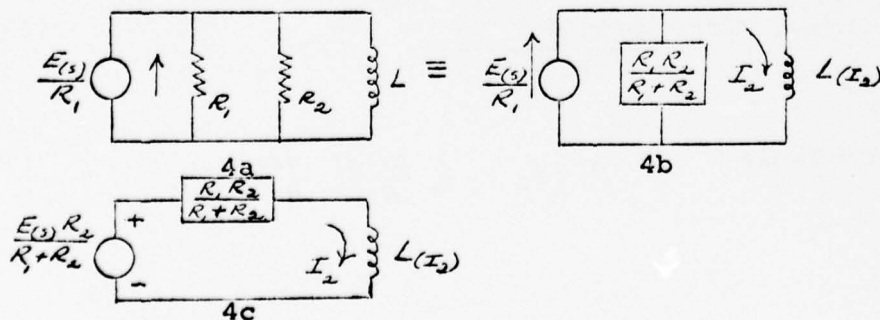
Fig. 3-23 Analyses Using Equivalent Circuits

68

Next find the parallel equivalent of R_1 and R_2 (Fig.3-23b) and then convert back to an equivalent voltage source (Fig. 4c). From Fig.3-23C one obtains directly the differential equation describing the magnetizing current as

$$\frac{d\,i_2}{dt} = \frac{\dfrac{e_{(t)}R_2}{R_1+R_2} - \dfrac{R_1 R_2}{R_1+R_2}\,i_2}{L(i_2)} \tag{81}$$

which verifys Equation (68).

Additional Dynamics - Series Leakage Reactance

The next step is to modify the circuit to account for an equivalent series leakage reactance. (Refer to Fig.3-24 where L_1 has been added.)
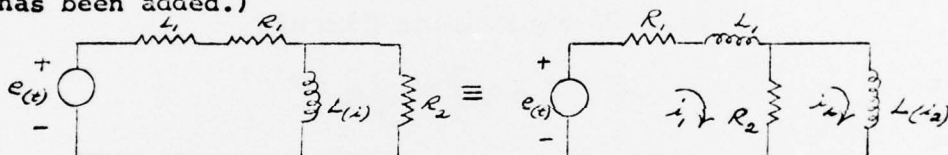
Fig.3-24 Leakage Reactance Added

Ladder analysis can now be applied, given that the proper interpretation of $L_{(i_2)}S$, as an operator on $I_{2(s)}$ alone, is observed.

Table 7   Ladder Analysis - Series Leakage Reactance

From Table 7, the ratio of I_2 (the magnetizing current) to E_0 is

$$\frac{I_2}{E_0} = \frac{1}{\left[\dfrac{L_1 s + R_1}{R_2}+1\right]L_2(I_2)S + L_1 s + R_1} \tag{82}$$

69

$$L_2(I_2)SI_2 + \frac{R_2(L_1S+R_1)}{L_1S+(R_1+R_2)} I_2 = \frac{E_{(s)}R_2}{L_1S+R_1+R_2} \qquad (83)$$

Let

$$Z_{eq} = \frac{R_2(L_1S+R_1)}{L_1S+R_1+R_2} = \frac{R_1R_2}{R_1+R_2} \frac{\left[\frac{L_1}{R_1}S+1\right]}{\left[\frac{L_1}{R_1+R_2}S+1\right]} \qquad (84)$$

$$E_{eq} = \frac{E_{(S)}R_2}{L_1S+R_1+R_2} = \frac{E_{(s)}R_2}{R_1+R_2} \left[\frac{1}{\frac{L_1}{R_1+R_2}S+1}\right] \qquad (85)$$

The equivalent circuit is given in Fig. 3-25.
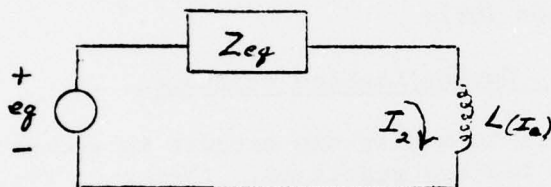
Fig. 3-25 Equivalent Circuit

Let

$$\mathcal{L}^{-1}\left[Z_{eq}\right] = Z_{eq}(t) \qquad (86)$$

$$\mathcal{L}^{-1}\left[E_{eq}\right] = e_{eq}(t) \qquad (87)$$

so that the differential equation, describing the magnetizing current, becomes

$$L(i_2)\frac{di_2}{dt} = e_g(t) - \int_0^t Z_{eq}(t-x)\,i_2(x)\,dx \qquad (88)$$

or

$$\frac{di_2}{dt} = \frac{e_{eq}(t) - \int_0^t Z_{eq}(t-x)\,i_2(x)\,dx}{L(i_2)} \qquad (89.)$$

The precise form of Equation (89) depends on the assumed values of the parameters. For example, as $R_2 \to \infty$, $E_{eq} \to E_{(s)}$ and $Z_{eq} \to R_1$. On the other hand, when $R_2 \ll R_1$,

$$E_q \to \frac{ER_2}{R_1} \frac{1}{\left[\frac{L_1}{R_1}S+1\right]} \qquad (90)$$

and

$$Z_{eq} \to \frac{R_1R_2}{R_1+R_2} \qquad (91)$$

70

For this important case, Equation (89) reduces to

$$\frac{di_2}{dt} = \frac{e_{eq}(t) - \left(\frac{R_1 R_2}{R_1 + R_2}\right) i_2}{L(i_2)} \tag{92}$$

and where $e_q(t)$ is dependent on the form of the assumed voltage. Given that $e(t) = V_0 \sin \omega t$ then

$$e_q = \frac{V_0 \omega}{s^2 + \omega^2} \cdot \frac{R_2}{R_1} \quad \frac{1}{\left[\frac{L_1}{R_1} s + 1\right]} \tag{93}$$

$$= \frac{V_0 \omega}{(s^2 + \omega^2)} \cdot \frac{R_2}{L_1} \cdot \frac{1}{s + R_1/L_1} \tag{94}$$

$$= \frac{As}{s^2 + \omega^2} + \frac{B(\omega)}{s^2 + \omega^2} + \frac{C}{s + R_1/L_1} \tag{95}$$

Therefore,

$$e_q(t) = A \cos \omega t + B \sin \omega t + C e^{-R_1/L_1 \, t} \tag{96}$$

$$\left. \begin{array}{l} A = -C = \dfrac{R_2 L_1 V_0 \omega}{(\omega L_1)^2 + R_1{}^2} \\[12pt] B = \dfrac{V_0 R_2}{R_1} \left[\dfrac{R_1{}^2}{(\omega L_1)^2 + R_1{}^2}\right] \end{array} \right\} \begin{array}{c} (97) \\[18pt] (98) \end{array}$$

In general, $e_q(t)$ will still have the form given in Equation (96) when both R_1 and R_2 are retained. However, the coefficients of the partial fraction expansion will be different. Specifically,

$$\left. \begin{array}{l} A = -C = \dfrac{R_2 L_1 V_0 \omega}{(\omega L_1)^2 + (R_1 + R_2)^2} \\[16pt] B = \dfrac{V_0 R_2}{R_1 + R_2} \left[\dfrac{(R_1 + R_2)^2}{(\omega L_1)^2 + (R_1 + R_2)^2}\right] \end{array} \right\} \tag{99}$$

Note that the increase in the "order" of the equivalent voltage source, due to the introduction of the energy storage element L_1 does not particularly complicate the problem. That is, the effect of L_1 on $e_q(t)$ can be treated in an analytical fashion - there is no need to "simulate" the complicating effects of L_1 as far as the equivalent source is concerned.

The effect of L_1 on the equivalent impedance is, however more involved and does theoretically require that we increase the order of the simulation model. Referring to Equation (84), observe that the equivalent impedance approaches

71

Fig. 3-17

58

a constant value, for all frequencies, only for two cases:
a) $R \to \infty$ b) $R_2 \to 0$. For the intermediate range where
$R_1 \simeq R_2$ it becomes necessary to find the exact "impulse re-
sponse" of $Z_{(s)}$. To find out what this impulse response is,
write Equation (84) in rational form (i.e., the ratio of
polynomials with the numerator polynomial of one order less
than the denominator):

$$Z_{eq} = \frac{R_1 R_2}{R_1 + R_2} \frac{\left[\frac{L_1}{R_1}s + 1\right]}{\left[\frac{L_1}{R_1+R_2}s + 1\right]} = R_2 \frac{s + R_1/L_1}{s + \frac{R_1+R_2}{L_1}} \tag{101}$$

$$= R_2 \left[1 - \frac{R_2/L_1}{s + \frac{R_1+R_2}{L_1}} \right] \tag{102}$$

$$\therefore \; Z_{eq}(t) = R_2 \, \delta(t) - \frac{R_2}{L_1} e^{-(R_1+R_2)t} \tag{103}$$

Using Equation (103) and Equation (96), Equation (89)
becomes
$$\frac{di_2}{dt} = \frac{(A\cos wt + B\sin wt + Ce^{-R_1/L_1 t}) - \int_0^t [R_2 \delta(t-x) - \frac{R_2^2}{L_1} e^{-\frac{R_1+R_2}{L_1}(t-x)}] i_2(x) dx}{L(i_2)} \tag{104}$$

Equation (104) simplifies only slightly:

$$\frac{di_2}{dt} = \frac{(A\cos wt + B\sin wt + Ce^{-R_1/L_1 t}) - R_2 i_2(t) + \frac{R_2^2}{L_1}\int_0^t e^{-\frac{R_1+R_2}{L_1}(t-x)} i_2(x) dx}{L(i_2)} \tag{105}$$

Let   (106)
$$W = \frac{R_2^2}{L_1}\int_0^t e^{-\frac{(R_1+R_2)}{L_1}(t-x)} i_2(x) dx$$

so that
$$\frac{dW}{dt} = \frac{R_2^2}{L_1} i_2 - \frac{(R_1+R_2)}{L_1} W \tag{107}$$

Thus Equation (105) can be replaced by the system of equations

$$\frac{di_2}{dt} = \frac{A\cos wt + B\sin wt + Ce^{-R_1/L_1 t} - R_2 i_2 + W}{L(i_2)} \tag{108}$$

$$\frac{dW}{dt} = \frac{R_2^2}{L_1} i_2 - \frac{(R_1+R_2)}{L_1} W \tag{109}$$

This system of equations has been programmed for the HP9830
and works well when $R_1 \simeq R_2$ and L has a reasonable numerical

value – on the order of 10^{-3} henrys. However, for L_1 on the order of 10^{-8} henrys the HP9830 underflows. Hence the use of Equation (96) is recommended only when L_1 has a significant value. This condition can be checked quite nicely using Equation (84). Note that Equation (84) gives the form

$$Z_{eq} = \frac{R_1 R_2}{R_1 + R_2} \left[\frac{\frac{L_1}{R_1} S + 1}{\frac{L_1}{R_1 + R_2} S + 1} \right] \tag{110}$$

or

$$Z_{eq} = \frac{R_1 R_2}{R_1 + R_2} \left[\frac{\frac{S}{\omega_1} + 1}{\frac{S}{\omega_2} + 1} \right] \tag{111}$$

We may compare the break frequencies ω_1 and ω_2 against the frequency of the input sine wave $V_0 \sin \omega t$. If $\omega_1, \omega_2 \gg \omega$ then we may as well set

$$Z_{eq} \equiv \frac{R_1 R_2}{R_1 + R_2} \tag{112}$$

In this event, Equation (89) becomes

$$\frac{di_2}{dt} = \frac{(A \cos \omega t + B \sin \omega t + C e^{-\frac{R_1}{L_1} t}) - \left(\frac{R_1 R_2}{R_1 + R_2}\right) i_2}{L(-2)} \tag{113}$$

Therefore, the program devised for Figure 3-20 (Equation (60) can be used by letting

$$e(\tau) \rightarrow A \cos 2\pi \tau + B \sin 2\pi \tau + C e^{-\frac{R_1}{L_1 F_0} \tau} \tag{114}$$

$$R \, i(\tau) \rightarrow \frac{R_1 R_2}{R_1 + R_2} \, i_2(\tau) \tag{115}$$

where

$$A = -C = \frac{R_2 L_1 V_0 \omega}{(\omega L_1)^2 + (R_1 + R_2)^2} \tag{116}$$

$$B = \frac{V_0 R_2}{R_1 + R_2} \left[\frac{(R_1 + R_2)^2}{(\omega L_1)^2 + (R_1 + R_2)^2} \right] \tag{117}$$

A More Detailed Model

Consider Fig 3-26 which makes provision for capacitive reactances as well as inductive losses. (We draw a frequency domain circuit diagram.)
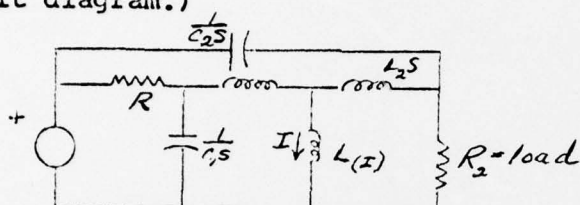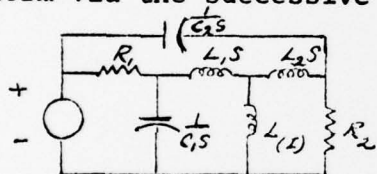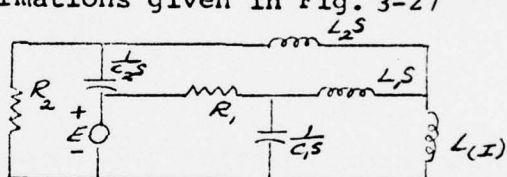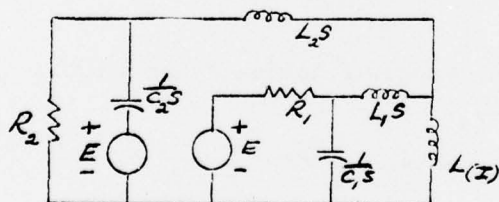

Fig.3-26A More Comprehensive Equivalent Circuit

This circuit can be reduced to the nonlinear first order form via the successive transformations given in Fig. 3-27
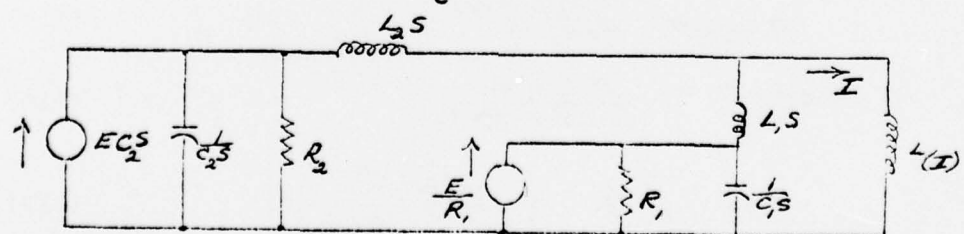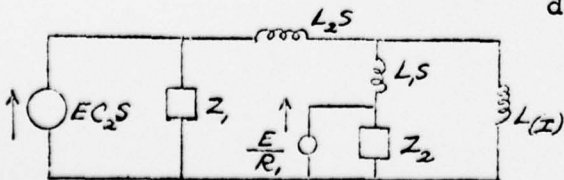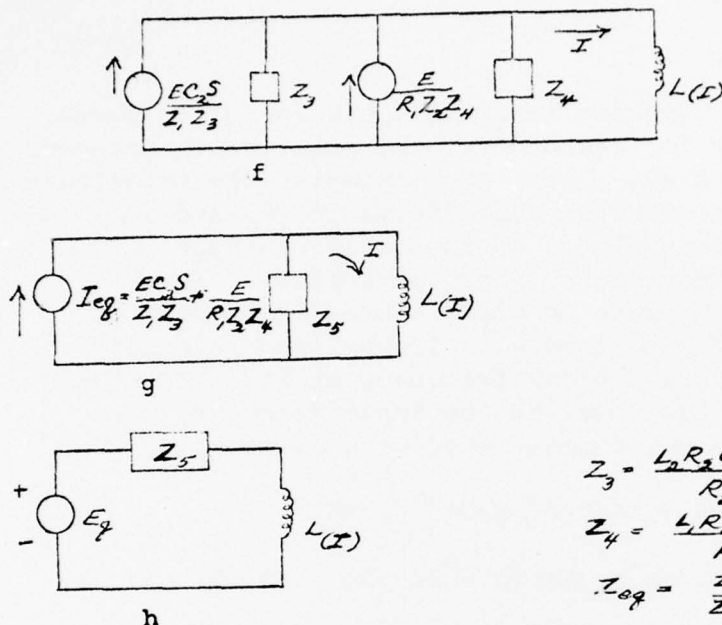

$$Z = \frac{R_2}{R_2 C_2 s + 1}$$

$$Z_2 = \frac{R_1}{R_1 C_1 s + 1}$$

Fig.3-27 Reduction of Fig 3-26 To First Order Form of Fig. 3-20

74

f

g

h

$$Z_3 = \frac{L_2 R_2 C_2 S^2 + L_2 S + R_2}{R_2 C_2 S + 1} \quad (119)$$

$$Z_4 = \frac{L_1 R_1 C_1 S^2 + L_1 S + R_1}{R_1 C_1 S + 1} \quad (120)$$

$$Z_{eq} = \frac{Z_3 Z_4}{Z_3 + Z_4} \quad (121)$$

Fig. 3-27 (con't)   Reduction of Fig. 3-26 to First Order Form of Fig. 3-27

Letting
$$Z_{eq}(t) = \mathcal{L}^{-1}\left[Z_{5(s)}\right] \quad (122)$$

and
$$e_{eq}(t) = \mathcal{L}^{-1}\left[E\left(\frac{C_2 S}{Z_1 Z_3} + \frac{1}{R_1 Z_2 Z_4}\right)\right] \quad (123)$$

gives the first order form
$$\frac{di}{dt} = \frac{e_{eq}(t) - \int_0^t Z_{eq}(t-\tau)\,i(\tau)\,d\tau}{L(i)} \quad (124)$$

Substituting the equivalent impedances into Equations (122) and (123) gives explicit expressions for $Z_{eq(s)}$ and $E_{eq(s)}$:

$$Z_{eq} = \frac{R_1 R_2}{R_1 + R_2} \; \frac{(T_1 T_3 S^2 + T_3 S + 1)(T_2 T_4 S^2 + T_4 S + 1)}{T_1 T_2 T_5 S^3 + T_5(T_1 + T_2)S^2 + \left[T_3 + \frac{R_1}{R_1 + R_2}T_2 + \frac{R_2}{R_1 + R_2}T_1\right]S + 1} \quad (125)$$

$$E_{eq} = \frac{E R_2}{R_1 + R_2} \; \frac{T_1 T_2 T_5 S^3 + T_2(T_2 + T_4)S^2 + (T_4 + \frac{R_1}{R_2}T_3)S + 1}{T_1 T_2 T_5 S^3 + T_5(T_1 + T_2)S^2 + \left[T_5 + \frac{R_1}{R_1 + R_2}T_2 + \frac{R_2 T_1}{R_1 + R_2}\right]S + 1} \quad (126)$$

where
$$T_1 = R_1 C_1 \quad , \quad T_2 = R_2 C_2 \quad (127)$$

$$T_3 = L_1 / R_1 \quad T_6 = L_1 / R_2 \quad (128)$$

75

$$T_4 = \frac{L_2}{R_2} \qquad T_5 = \frac{L_1 + L_2}{R_1 + R_2}$$

(129)

One may evaluate quation (125) and (126), for given para-
meter values, and check for resonances, the relative importance
of each term in Z_{eq} and E_{eq}, etc. For example, the importance
of the various break frequencies encountered in Z_{eq} and E_{eq}
can be assessed using Bode plots, on the basis of their
relavance to the frequency of the input sinusoidal. For
example, if Equation 125 were to yield a break frequency at
5000 HZ we would choose to ignore it if the input sinusoid
were at 60 HZ. However, a break frequency at 5000 HZ would
have to be retained in the model if the input frequency were
1000 HZ. These points are demonstrated with an example. Let

$$f_0 = 60 HZ, \quad R = .01, \quad R_2 = .001, \quad L_1 = L_2 = 10^{-6}, \quad C_1 = 10^{-8}, \quad C_2 = 10^{-4}$$

Using these numbers, it can be shown that Z_{eq} and E_{eq} can be
factored explicitly as

$$Z_{eq} = \frac{R_1 R_2}{R_1 + R_2} \cdot \frac{(T_1 S + 1)(T_3 + 1)(T_2 S + 1)(T_4 S + 1)}{(T_1 S + 1)(T_2 S + 1)(T_3 S + 1)}$$

(130)

$$= \frac{R_1 R_2}{R_1 + R_2} \cdot \frac{(T_3 S + 1)(T_4 S + 1)}{(T_5 S + 1)} = 9.091 \times 10^{-4} \cdot \frac{\left(\frac{S}{10000} + 1\right)\left(\frac{S}{1000} + 1\right)}{\left(\frac{S}{549} + 1\right)}$$

$$\text{and} \quad E_{eq} = \frac{E R_2}{R_1 R_2} \cdot \frac{(T_1 S + 1)(T_2 S + 1)(T_4 S + 1)}{(T_1 S + 1)(T_2 S + 1)(T_3 S + 1)} \quad .$$

(131)

$$\frac{E_{eq}}{E} = \frac{R_2}{R_1 + R_2} \cdot \frac{(T_4 S + 1)}{(T_5 S + 1)} = .091 \frac{\left(\frac{S}{1000} + 1\right)}{\left(\frac{S}{5494} + 1\right)}$$

(132)

Since the input frequency is 377 rad/sec, the break fre-
quencies of Equations (130) and (131) are of no concern and we may
as well set

$$Z_{eq} = \frac{R_1 R_2}{R_1 + R_2}$$

(133)

$$\text{and} \quad E_{eq} = \frac{E R_2}{R_1 + R_2}$$

(134)

Load current and magnetizing current are plotted in Figs. 3-28
and 3-29 for two different values of input voltage (V=3 and
V=5). In addition, the spectral content of the load current,
for the V=5 case, is examined in Fig. 3-30

In both cases (V=3, V=5), the following parameter values
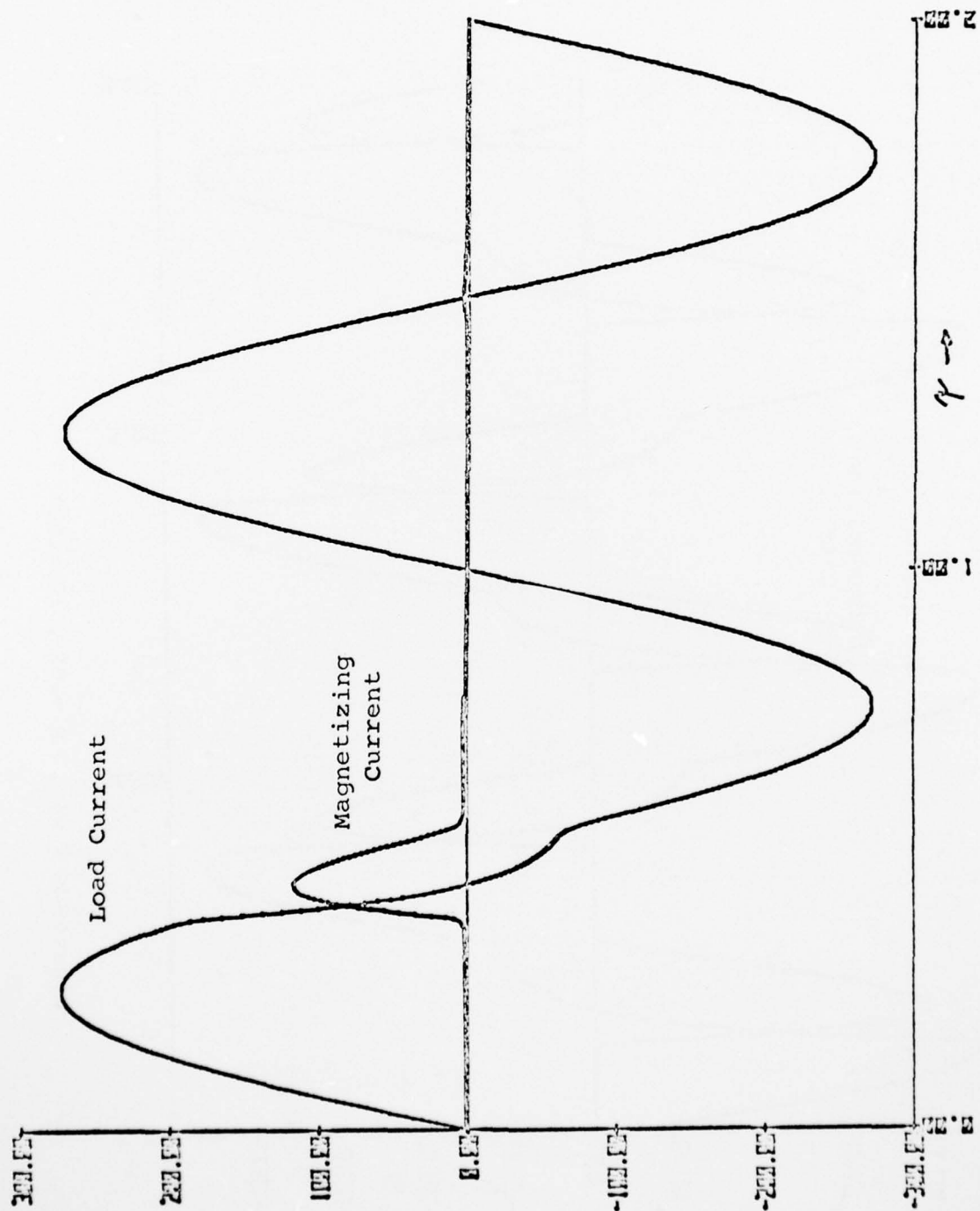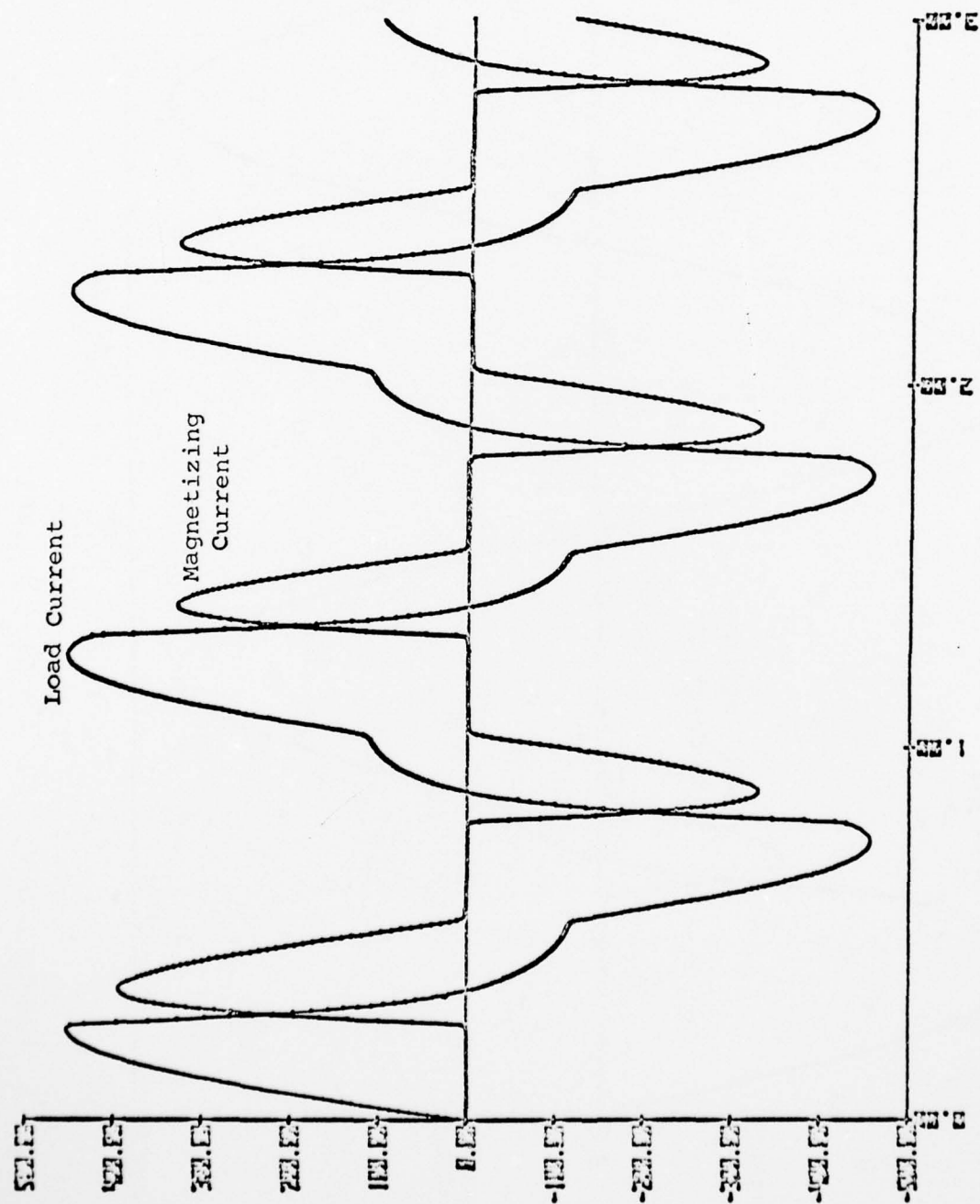were used for the nonlinear model:

76

Figure 3-28 V = 3, R = .01 R = .001

77

Figure 3.29 V = 5 , R = .01 , R = .001

78
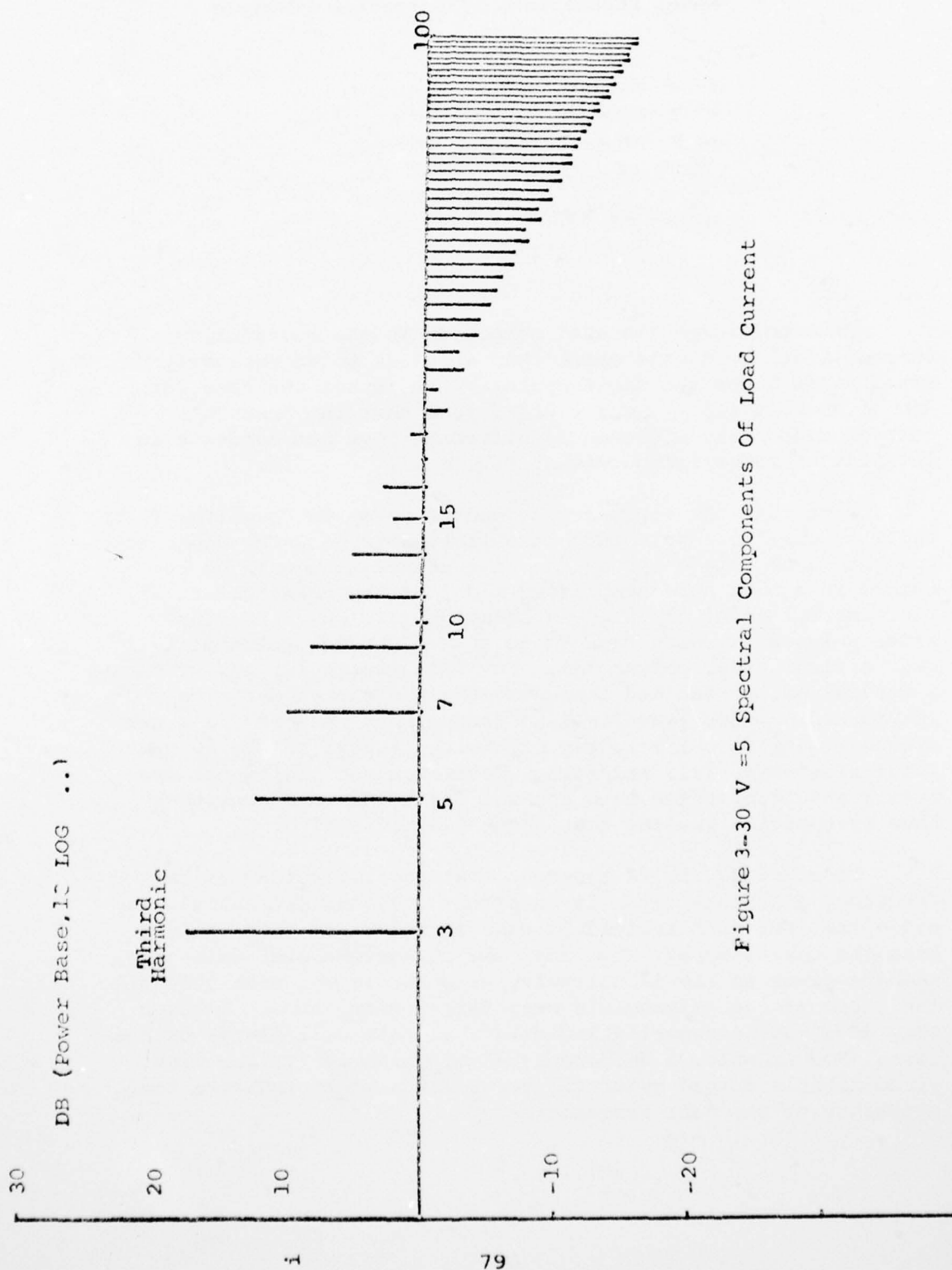
Figure 3–30 V = 5 Spectral Components Of Load Current

79

TABLE 8

Model Parameters, Illustrative Example

$$N = 100$$
$$A_c = 4.3 \times 10^{-6} \, m^2$$
$$\ell = 8.47 \times 10^{-2} \, m$$
$$\mu_o = 4\pi \times 10^{-7} \, H/m$$
$$B_s = 1.8 \, T$$
$$B_u = 1 \, T$$
$$H_c = 40 \, A/m$$

Note the large "inrush" component in the magnetizing current (for the 3 volt case) that dies out to an extremely small value after the first cycle. This is not the case for the V_o =5 volt input - there it is seen that the "inrush" current component, although significant, does not dominate in the plot of magnetizing current vs. τ .

Note that the frequency dependent terms in Equations (125) and (126 exhibit a pole-zero cancellation trend which seems to indicate that only a few of the time constants should be retained in a much more simplified model of the transformer. That is, the model of Z_{eq} in Equation (125) was a fourth order polynomial which reduced to a second order polynomial over a first order polynomial. For this particular set of parameter values, we decided to ignore the additional dynamics introduced by this lead-lag-lead factor only because the break frequencies were sufficiently high with respect to the 60 Hz input sine wave. (377 rad/sec). However, these additional dynamics should be taken into account for input waveforms that have frequencies greater than about 600 rad/sec.

To conclude, it is apparent that the importance of the frequency dependent terms in Equations (125) and (126) should be evaluated. for each individual case in order to gain insight into the character of Z_{eq} and E_{eq} . For example, using the numbers given in the illustrative example, it was seen that all the roots of the polynomials were first order terms. However, this does not necessarily indicate that this will always be the case. For example, a different set of parameter values might yield lightly damped quadratic terms which would indicate the existance of resonant frequencies.

3.4   200KW Transformer

The original plan was for the 200KW system to be a scaled-up version of the 10KW system. At the time, it was not known what the effect of nonlinear characteristics would be on this intended scaling. In fact one of the program objectives was to determine the extent and predictability of these nonlinearities. As the work progressed, it became evident that direct scaling was not possible. This being the case, some preliminary 200KW designs were run with resulting system specific weights of less than 0.1 lb/KVA. The 10KW test results will contribute to the establishment of coil separation and interleaving requirements of the 200 KW unit. Detailed design of this unit will follow and final 10KW transformer/rectifier fabrication and testing.

4.0   Conclusions

The program is proceeding on schedule. Valuable information has been obtained from the 10KW fabrication and testing which has permitted the elimination of several inaccuracies in the computer programs, and the addition of certain new features such as "pie" winding design capability. New techniques for the fabrication of lightweight "pie"windings have been developed which show great promise. Several prototype 10KW units have been completed and subjected to preliminary testing. A 10KW water cooled T/R unit will be completed in August 1976 as scheduled.

Several improvements were made in the magnetic core model which permit the accurate simulation of hysteresis and I-V curves for most core materials. A procedure was developed for determining the complete dynamic behavior of any transformer which can be represented by lumped parameters and the nonlinear core model. This procedure yields both time dependent characteristics and harmonic content. It requires that all of the transformer characteristics be specified.

The 200 KW transformer design should proceed without difficulty after the 10KW unit is complete.

81

REFERENCES

1. Tape Wound Bobbin Cores - Arnold Engineering Catalog TC-108C
2. Power Transformer and Inductor Design - Magnetics Inc. TID-100
3. Tape Wound Cores - Arnold Engineering Catalog TC-101B
4. Inverter Transformer Core Design and Material Selection-
    Col. Wm. T. McLyman - JPL
5. Staff-Thermal Technology Laboratory Inc. Final Report
    USAF Contract No. F33615-75-C-1944
6. Manly, Wm. A. Jr. " An appraisal of several nonlinear
    hysteresis loop models" IEEE Trans. on Magnetics,
    Vol. MAG-9, No. 3, Sept. 1973
7. MacFadyen, W.K., Simpson, R.R.S., Stater, R.D. and Wood, W.S.
    "Representation of magnetisation curves by exponential series"
    Proc. IEE, 1973, Vol 120 No. 8, PP 992-994
8. Widger, G.F.T. "Representation of magnetisation curves
    over extensive range by rational-fraction approximations",
    Proc. IEE, 1969, Vol.116, No.1, PP 156-160
9. Nitzan, D., "MTRAC: Computer program for transient analysis
    of circuits including magnetic cores" IEEE Trans. on
    Magnetics, Vol. MAG-5, No.3, Sept. 1969